

Review

# On the Sustainable Utilization of Geopolymers for Safe Management of Radioactive Waste: A Review

Esther Phillip <sup>1</sup>, Thye Foo Choo <sup>1</sup>, Nurul Wahida Ahmad Khairuddin <sup>1</sup> and Rehab O. Abdel Rahman <sup>2,\*</sup><sup>1</sup> Malaysian Nuclear Agency (Nuclear Malaysia) Bangi, Kajang 43000, Selangor, Malaysia<sup>2</sup> Hot Laboratory Center, Atomic Energy Authority of Egypt, Cairo 13759, Egypt

\* Correspondence: alaarehab@yahoo.com; Tel.: +20-10-6140-4462

**Abstract:** The application of geopolymers for the safe management of radioactive waste has not been implemented on a large scale, where they are tirelessly examined with the purpose of facilitating the practicality and feasibility of the actual application towards the sustainable performance of these materials. This review therefore compiles the findings of the utilization of geopolymers as sorbents for removal of radio-contaminants from aqueous waste streams and as immobilization matrices for the containment of different radioactive wastes. The investigated geopolymer base materials encompass a wide range of reactive aluminosilicate precursor sources that include natural materials, industrial wastes, and chemicals. This work introduces to the reader the scientific interest in the field of geopolymer studies, their sustainability analysis, and their application in the nuclear industry, in particular in radioactive waste treatment and immobilization. The geopolymer classification, radiation stability, and structural characterizations were summarized with special reference to the characterization of the structure alteration due to the inclusion of functional materials or radioactive wastes. The effect of the application of metakaolin-based materials, fly ash-based materials and other base materials, and their blend on radio-contaminant removal from aqueous solutions and the immobilization of different problematic radioactive waste streams were reviewed and analyzed to identify the gaps in the sustainable performance of these materials. Finally, perspectives on geopolymer sustainability are presented, and the identified gaps in sustainable application included the need to investigate new areas of application, e.g., in pretreatment and membrane separation. The reusability and the regeneration of the geopolymer sorbents/exchangers need to be addressed to reduce the material footprints of this application. Moreover, there is a need to develop durability tests and standards based on the record of the application of the geopolymers.

**Keywords:** geopolymers; radioactive waste; sorbent; immobilization matrices; performance measures



**Citation:** Phillip, E.; Choo, T.F.; Khairuddin, N.W.A.; Abdel Rahman, R.O. On the Sustainable Utilization of Geopolymers for Safe Management of Radioactive Waste: A Review. *Sustainability* **2023**, *15*, 1117. <https://doi.org/10.3390/su15021117>

Academic Editor: Changhyun Roh

Received: 17 November 2022

Revised: 27 December 2022

Accepted: 3 January 2023

Published: 6 January 2023



**Copyright:** © 2023 by the authors. Licensee MDPI, Basel, Switzerland. This article is an open access article distributed under the terms and conditions of the Creative Commons Attribution (CC BY) license (<https://creativecommons.org/licenses/by/4.0/>).

## 1. Introduction

In nuclear industry, large quantities of radioactive effluents are generated by nuclear power plants [1], hospitals and medical and research laboratories [2], as well as nuclear accidents [2,3]. The volumes of the stored effluents are dependent on the size and nature of the national nuclear program, which was reported to fall in the range of few tens to ten of thousands of cubic meters [4]. The main contaminants of concerns in these effluents include,  $^3\text{H}$ ,  $^{60}\text{Co}$ ,  $^{85}\text{Kr}$ ,  $^{131}\text{I}$ ,  $^{133}\text{Xe}$ ,  $^{134}\text{Cs}$ ,  $^{137}\text{Cs}$  and  $^{90}\text{Sr}$  [1]. These radioactive effluents need to be managed safely to ensure the protection of human health and to minimize their environmental impacts. The radiological, chemical, physical, and biological characteristics of these effluents are dependent on the generating process, and these characteristics determine the selected waste treatment route that usually necessitates the use of combined treatment technologies. Various chemical treatment technologies are widely employed to reduce the volume of these effluents. Examples of these technologies include membrane separation [5,6], coagulation [7], electrochemical precipitation [8–11], and sorption/ion

exchange [12–14]. After the treatment, the treated effluents are discharged or reused according to the adopted procedure at the treatment facility and the exhausted materials and/or produced sludge are managed as radioactive wastes. Among these technologies, sorption/ion exchange is more common and widely used. The studies in this field are directed to develop assorted sorbent materials such as modified clay [15], zeolite [16], synthetic polymer [17], cellulose [18], and geopolymer [19–28] to ensure the effective removal of radionuclides from aqueous solutions. In addition to these effluents, organic liquid wastes are generated due to the operation of nuclear fuel cycle and some medical research facilities and research laboratories. The volumes of these organic liquid wastes are relatively small compared to those of the effluents [29]. These wastes have varying radiological, biological, and chemical characteristics and require special treatment that includes the application of non-destructive, direct immobilization or destructive methods, refs. [29–33]. In non-destructive treatment, the organic content remains intact, and physical changes in the waste properties are targeted. Absorption is widely applied as a non-destructive method to treat spent lubricants and solvents; this process does not aim to reduce the volume of the wastes, but it aims to improve the subsequent immobilization practice [30,31]. Drying and evaporation are non-destructive methods that are applied to reduce the volume of the generated organic solvents, and the resultant concentrates are managed as radioactive wastes. Direct immobilization is used to manage the spent ion-exchangers and organic liquids [30,31,33]. Finally, the destructive treatment of the organic wastes involves chemical changes in the waste that leads to considerable volume reduction in comparison with the previously mentioned methods. These methods include thermal, chemical, and biological treatments; the first, e.g., incineration and plasma treatment, are employed to treat spent solvents and lubricants. The ashes produced from these methods are sent for immobilization, and the off-gases are treated [29–31]. The chemical and biological treatments are also applied for the treatment of the organic liquid wastes, and the resultant sludge is managed as radioactive wastes, and the off gases are treated [29–31].

After treatment, hazardous wastes, including radioactive wastes, are recommended to be immobilized in a suitable matrix to ensure their containment [34]. This method involves confining the radioactive waste within a binder material to produce a stable wasteform that complies with specified requirements on their durability. The wasteforms can effectively reduce the mobility of radionuclides by physical encapsulation, sorption, or chemical interaction processes [35]. At present, the immobilization of different radioactive wastes has been achieved using several types of binders, including ceramics [36–39], glasses [40,41], conventional and innovative cement-based materials [31–33,42–63], bitumens [64,65], and polymers [66,67]. Ceramic wasteforms include variable chemical structures, e.g., simple oxides with a fluorite structure; complex oxides; simple silicates; and silicate, phosphate, and aluminate frameworks [36]. They are used to immobilize nuclear wastes. Phosphate and borosilicate glasses are widely employed to immobilize nuclear wastes, and in some cases, they were applied to low- and intermediate-level radioactive waste immobilization [39,40]. Conventional cement-based wasteforms relied on the use of ordinary Portland cement (OPC), with or without additives, as an immobilization matrix, whereas the innovative cements include calcium aluminate cements (CAC), calcium sulfo-aluminate cements (CSAC), magnesium phosphate cements (MPC), and alkali-activated cements (AAC) [31,32]. Cement-based wasteforms are widely used to immobilize different types of low- and intermediate-level radioactive wastes. Bitumens and polymers have been used as immobilizing media for the encapsulation of low- and intermediate-level radioactive wastes; they can be optimized to allow high waste loading and good retention characteristics [31,42].

Geopolymers are inorganic materials that are produced by low-temperature polymerization of an aluminosilicate precursor in an alkaline solution [68]. It was known as soil cement, inorganic polymer, then was named as geopolymer by Joseph Davidovits in 1978 [31]. This relatively innovative class of materials received wide scientific interest to develop various applications in a vast array of industrial sectors. This interest has

tremendously increased within the last decade; an unrestricted analysis of Scopus database using the keyword “Geopolymer” was recently conducted on 8 October 2022, showing that there were 39,115 published items in that database; nearly two thirds of these works were published in the prior 4 years (Figure 1a). According to the analysis of the data, review papers published in this field represents only 5.98% of the published work. Geopolymers find their applications as civil engineering materials [69], insulation materials [70], coating materials [71], ceramic materials [72], fire-resistance materials [73], catalysts [74], municipal-waste immobilization matrix [75], etc. These applications are supported by the reduced environmental impacts of these materials compared to conventional cement-based materials in terms of reduced energy consumption and CO<sub>2</sub> emissions. In addition, the economy of a geopolymer prepared from waste materials supports the transition from a linear to a circular economy. Subsequently, the sustainability of these materials received considerable scientific attention. Figure 1b illustrates the increasing scientific interest in addressing the sustainability of the geopolymer materials that represents nearly 19.11% of the total research in geopolymer. Most of the published works are research papers that represent the main contributing publication type for evaluating the geopolymers and their sustainability (Figure 1c,d). The review papers have increased contributions to the “geopolymer sustainability” publications compared to that of the “geopolymer” publications.

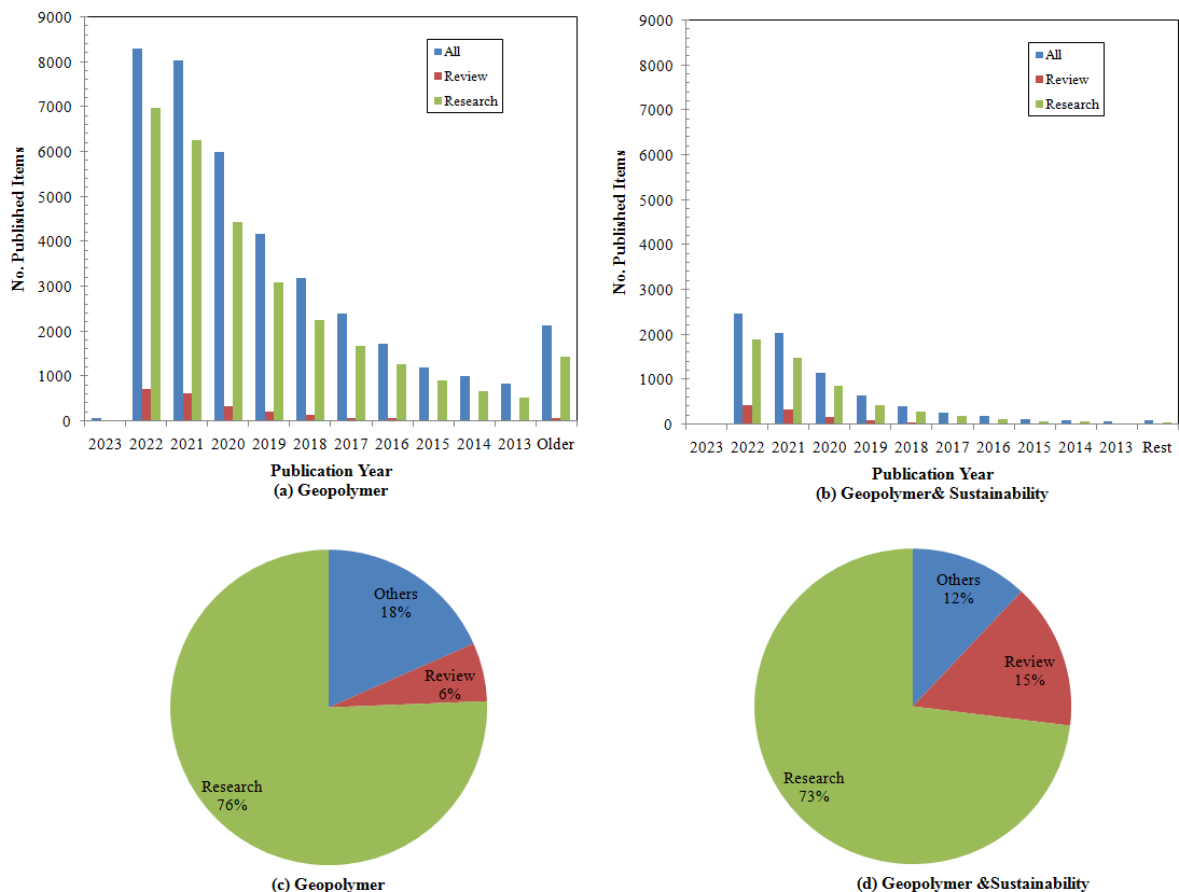


**Figure 1.** Bibliometric data analysis (a,b) number of annual scientific publications, (c,d) relative contribution of the research and review papers to the total published items that addressed geopolymers and geopolymer sustainability, respectively.

In the radioactive-waste-management field, geopolymers have also attracted considerable attention for their applications in the treatment and immobilization of these wastes. This is due to their many advantages, including low cost and simple preparation process, as well as good mechanical properties and thermal and chemical stability. By analyzing the

bibliometric data in Scopus database, there are 4460 publications that motioned the word “Geopolymer” AND “Nuclear”. Figure 2a (insert) shows the annual distribution of the published work that included both words in comparison with that related to “geopolymers” over that last decade. Both publication fields have exponential growing trends with a relatively higher exponential constant for the general field. The number of the publications that mentioned “Removal” was lower than those mentioned “Immobilization” until 2018, then this trend was reversed. The publications that mentioned “Nuclear” represent nearly 11% of the total geopolymers publications (Figure 2b). Overall of the analyzed data, there is a fairly equal contribution from the publications that mentioned “Removal” and “Immobilization” and from the total publications that motioned “Geopolymer” And “Nuclear” (Figure 2c). The addition of the word “Sustainability” reduces the numbers of the published work by nearly 15%, with a noted exponential increasing trend and with no clear pattern on the relative contribution of “Removal” and “Immobilization” to the annual published items (Figure 2d).

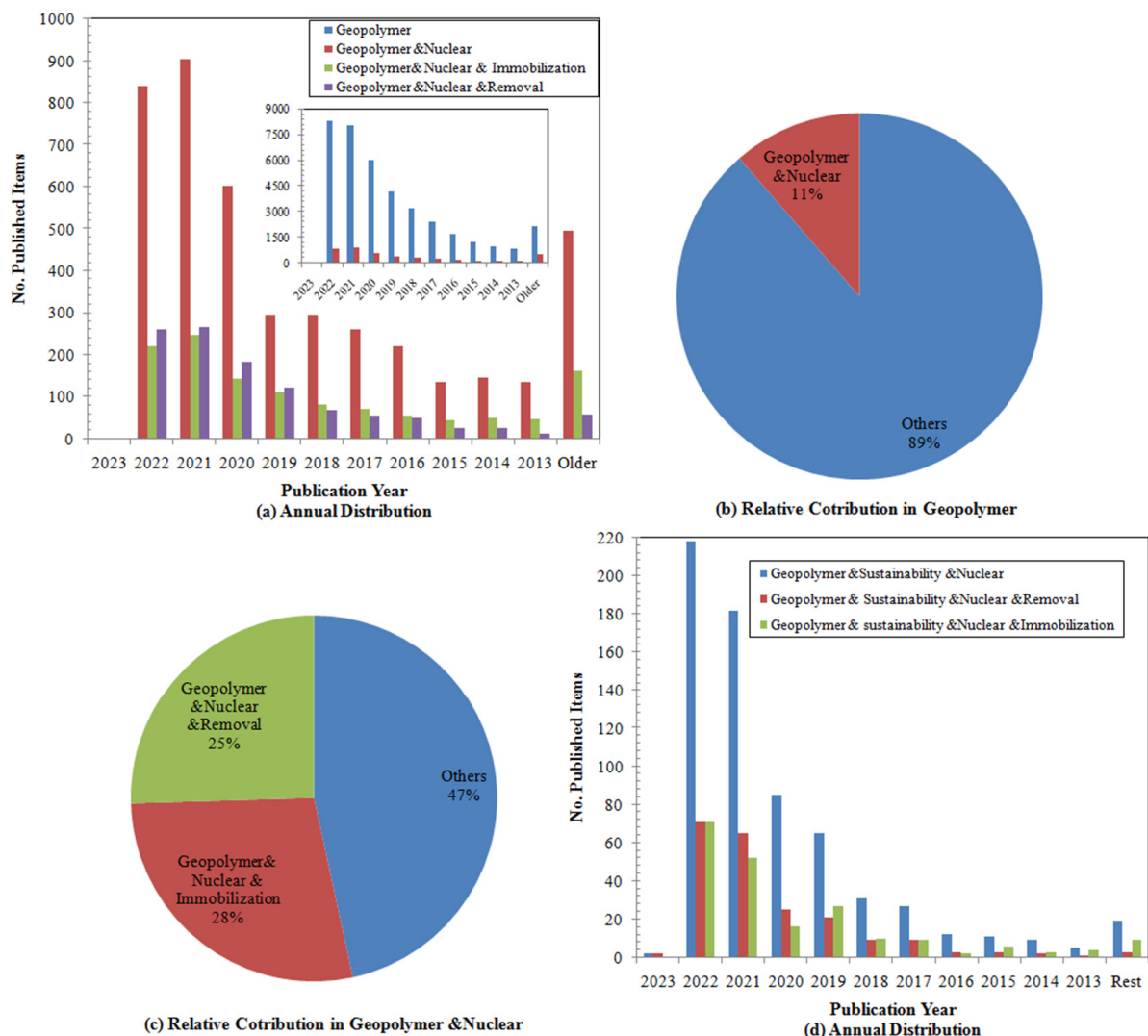


**Figure 2.** Bibliometric data analysis for publications that mentioned a combination of the words geopolymer, nuclear, removal, and immobilization. (a) Annual distribution during the last decade. (b) Relative contribution of “Geopolymer” and “Nuclear” to the geopolymer publications. (c) Relative contribution of the paper type to the total published work on nuclear and geopolymers. (d) Annual distribution of the papers that addressed the sustainability in this field.

The development of geopolymers for various applications has been widely reported in literature, and several comprehensive reviews have been published recently. Recent review papers were directed to assess the geopolymer synthesis, applications, and challenges, but only one addressed the sustainability of the geopolymer in environmental remediation [76–82]. Of these review papers, four papers were directed to cover the use of geopolymer in water and wastewater treatment [76,78–80]. Review papers that addressed the application of geopolymer materials in immobilization covered both the solidification/stabilization and removal applications for heavy metal [83–89], whereas only two review articles addressed it in the context of radioactive wastes [87,89], and one addressed the immobilization of organic liquid wastes in general [90]. However, none of these reviews was directed at discussing the integrated applications of geopolymers in radioactive waste management from the sustainability point of view. Thus, the objective of this paper is to compile and review various geopolymers, aiming to identify the gaps in the current knowledge about the sustainable performance of these materials. In particular, gaps towards the large-scale application of these materials as sorbents and gaps in identifying the factors that affect the durability of the geopolymer immobilization matrices will be addressed. In addition, areas that have not been addressed in radioactive waste management will be identified with reference to similar applications in the non-nuclear wastewater treatment field. In this context, the classification of geopolymers, their radiation stability, and their structure characterizations will be summarized with special reference to the geopolymers that have been tested as sorbent/immobilization matrix for radioactive wastes. Recent advances in testing different geopolymers for their applications as sorbents will be reviewed with a focus on the studied precursors and analyzing their performance in the removal of radio-contaminants from an aqueous solution. Similarly, the recent advances in testing the geopolymer immobilization matrices will be reviewed with a special focus on analyzing the sustainability of their safety function. Finally, a perspective on the sustainability of these materials will be presented.

## 2. Geopolymers

Geopolymers are a relatively new class of inorganic amorphous materials, which has recently been used in large-scale applications. The main ingredients to prepare geopolymers are reactive aluminosilicate precursor (named here as base material) and activating alkali solutions, e.g., NaOH, KOH, waterglass. The kinetics of geopolymerization to form a three-dimensional network structure of aluminates and silicates tetrahedrons are complex and include: dissolution, speciation equilibrium, gelation, reorganization, and polymerization and hardening [31,91]. The main binding phase in geopolymers is the aluminosilicate gel and is classified, based on its Si/Al ratio, into; poly(sialate) (Si/Al = 1), poly(sialate-siloxo) (Si/Al = 2), and poly(sialate-disiloxo) (Si/Al = 3) [92–94]. In comparison with zeolite structure, these Si/Al ratios correspond to low ( $\leq 2$ ) and intermediate ( $2 < \text{Si/Al} \leq 5$ ) silica zeolite [95]. The final properties of geopolymers are related to their microstructures, which are strongly dependent on the formulation and the nature of the base materials and the preparation and curing conditions [68]. General properties for these classes are as follows [31,96,97]:

- Si/Al < 1 noted zeolite crystallization is observed in geopolymers;
- $1 < \text{Si/Al} < 2$  increased polymerization degree, with reduced porosity;
- $2 < \text{Si/Al}$  the polymerization extent is dependent on the solubility of the Si source.

Based on the alkaline nature of the geopolymers and the ability of their structures to be tailored, this class of materials can be employed in various radioactive-waste-management activities as follows:

- Pre-treatment activity: Due to the high buffer capacity of these materials, geopolymers can be used to regulate the pH of the aqueous radioactive waste streams;
- Aqueous effluents treatment activity: Porous geopolymers composites can be used in membrane separation, sorption/ion exchange, filtration, and photocatalytic degradation;

- Immobilization activity: Impermeable geopolymers can be used in the direct immobilization of problematic operational waste streams, e.g., organic liquid wastes, spent ion-exchangers, and evaporated concentrates.

Up to now, scientific efforts have not covered all these applications in radioactive waste management. Most of the conducted work focused on the ability of the geopolymers to remove some radionuclides of concern via sorption/ion exchange or to immobilize the radioactive wastes in geopolymers [20–28,31,45–63,68–74,98–110]. In this section, an overview of the used materials in geopolymers preparation, the effect of the radiation on these materials, and techniques to characterize their structure are presented.

### 2.1. Base Materials

A large number of materials have been used as base materials (source for silica and alumina) to synthesize geopolymers; these materials can be classified into three groups:

- Natural minerals: These are the most popular structural elements sources for geopolymer synthesis. Calcined kaolin (CK)/metakaolin (MK) have been extensively tested to prepare sorbents [20,24,26–28,100,111] and immobilization matrices [35,45,46,48–50,52,53,55–62,101,103]. Limited research investigated other minerals, including feldspar (F), bentonite (B), and mordenite (M), for the same purposes [54,62,98,104,105].
- Industrial wastes: Fly ash (FA) is the most widely used waste in the preparation of geopolymer sorbents [21–23,25] and immobilization matrices [47,55,61,98,102,104,106]. Some research used blast furnace slag (BFS) with other materials to prepare sorbents [23–25] and geopolymeric immobilization matrices [50,51,55,61]. Manganese slag (MS) was employed to prepare immobilization matrices [45]. Prior to the utilization of these materials, they should be tested using toxicity characteristics leaching test (TCLP) to ensure that their heavy metal content, if any, is in stable form. Additionally, the amount of the natural occurring radioactive materials in these wastes should be quantified, if suspected.
- Synthetic materials: Chemical sodium silicate and aluminum nitrate solutions have been used to prepare sorbent material to test its potential application in radioactive metal removal from aqueous solutions [110]. In addition, Betol 39T was investigated to prepare geopolymer immobilization matrix [59].

### 2.2. Effect of Radiation on Geopolymers

Exposure to radiation can lead to various changes in the materials depending on their structures and exposure doses. Chemical changes can occur in materials due to the radiolysis reactions; the radiation chemical yield ( $G$ ,  $\mu\text{mol}/\text{J}$ ) is used to quantify the extent of these reactions and subsequently, the radiological stability of these materials. It is defined as the number of formed species due to the absorption of 100 eV. Physical changes can occur on the macro- and/or micro-scales, e.g., change in the volume [13], pore number, and structure [51]. These changes can affect the performance of the material and its life time. In order to assess the suitability of geopolymers for their applications in radioactive waste management, their radiological stability and durability should be assessed [112]. Several studies have closely examined the changes in geopolymers under gamma ( $\gamma$ ) irradiation. The studied parameters included the radiation chemical yield compressive strength ( $\sigma$ , MPa) as an indication for the changes in mechanical properties and cumulative leach fraction (CLF,  $\text{cm}^{-1}$ ) as an indicator for the stabilization performance of radionuclides within the immobilization matrix; a summary of these studies is shown in Table 1. Limited studies presented the effect of  $\gamma$ -radiation on MK and FA geopolymers by measuring the hydrogen chemical radiation yield under a wide range of exposure doses [101–103]. The hydrogen radiolytic yields were reported in the range of 2.1 to  $9.0 \times 10^{-3} \mu\text{mol}/\text{J}$  (Table 1); these values are lower than those reported for OPC cements ( $\sim 1.0 \times 10^{-2} \mu\text{mol}/\text{J}$ ) and pure bulk water ( $4.7 \times 10^{-2} \mu\text{mol}/\text{J}$ ) [105,106]. It should be noted that the yield is highly dependent on the water saturation in the sample and the exposure doses, which should be considered as a factor in these studies [113].

**Table 1.** Effect of gamma ( $\gamma$ ) irradiation on geopolymers: Hydrogen radiolytic yield, compressive strength, and leaching.

Geopolymer	Dose, kGy	Property	Effect	Ref.
GGBFS*/Wollastonite	1000	Compressive strength	$\Delta\sigma$ increased by 35%	[51]
MK	50	Hydrogen radiolytic	$G = 6.1 \times 10^{-3} \mu\text{mol/J}$	[101]
FA	700	Hydrogen radiolytic	$G = 2.1 \times 10^{-3} \mu\text{mol/J}$	[102]
MK	750	Hydrogen radiolytic	$G = 9.0 \times 10^{-3} \mu\text{mol/J}$	[103]
	50–1000	Compressive strength	$\Delta\sigma \sim 10\%$	
FA	100	Compressive strength	$\Delta\sigma 7.8\%$	[106]
		Radionuclide leaching	$\Delta\text{CLF } 5, 22.3 \text{ and } 47.3\%$ , in DIW **, GW *** & SW ****	

\* GGBFS granulated grounded BFS. \*\* DIW deionized water. \*\*\* GW ground water. \*\*\*\* SW seawater.

The results of investigating the effect of  $\gamma$ -radiation on the geopolymer compressive strength confirmed increased compressive strength after irradiation for doses in the range of 50 to 1000 kGy (Table 1) [51,103,106]. A change of about 10% after irradiation was reported at different doses in the range 50 to 1000 kGy for MK-based geopolymer; it was attributed to the densification in the geopolymer network structure [103]. For BFS-based geopolymers, a higher increase in the compressive strength of 35% was noted at an irradiation dose equal to 1000 kGy; this value was reduced progressively as the waste loading increased [51]. The increase in compressive strength under  $\gamma$ -radiation was attributed to the decrease in the mean Si–O–Si angle and the decrease in the average pore size of the geopolymer [51]. It should be noted that no significant change occurred due to the irradiation of the Fe-rich geopolymer prepared from synthetic plasma slag up to 5 kGy [114]. The irradiation of the geopolymer prepared from BSF/FA blend, up to 10,214 kGy, revealed that two competing mechanisms are responsible for the changes that occur in the geopolymer during the irradiation. The first is beneficial, enhancing the gelation and cross-linking of the geopolymer, and is dominant at lower irradiation doses. The second is detrimental; it causes structural and micro-structural destabilization and is dominant at higher irradiation doses [115]. The reported improvement in the compressive strength in Table 1 was associated with increases in the CLF, which is a negative change for the stabilization performance. This change in the CLF is highly dependent on the type of the leaching solution (Table 1). However, this increase in the CLF was reported as still complying with the acceptance criteria set by the American Nuclear Society Standards committee [106,116].

### 2.3. Geopolymer Structure Characterization

By default, geopolymers are amorphous aluminosilicate materials that can contain some crystalline phases embedded in it. These phases might be residual from the base material or due to the preparation of the geopolymer composite. In general, there are various techniques that can be employed to quantify the morphology, and the pore and chemical structure of the materials. The morphology is usually identified using microscopy techniques, e.g., optical, secondary electron microscope (SEM), and transmission electron microscope (TEM). Moreover, SEM and TEM can give information about the elemental distribution in the material and its crystal structure, respectively. Figure 3a illustrates the elemental distribution of the structural elements, i.e., Si, O, Al, and the immobilized contaminant, i.e., Cd, in a BFS-based geopolymer [117]. The uniform distribution of the contaminant in the geopolymer is an indication of the effective immobilization [117]. Figure 3b,c illustrates the inclusion of crystalline nano-particles in a MK-based geopolymer, wherein the dimensions of these inclusions can be measured from the TEM image, i.e., Figure 3b, and the d-spacing of the crystalline material can be determined from the electron diffraction pattern, i.e., Figure 3c [118].

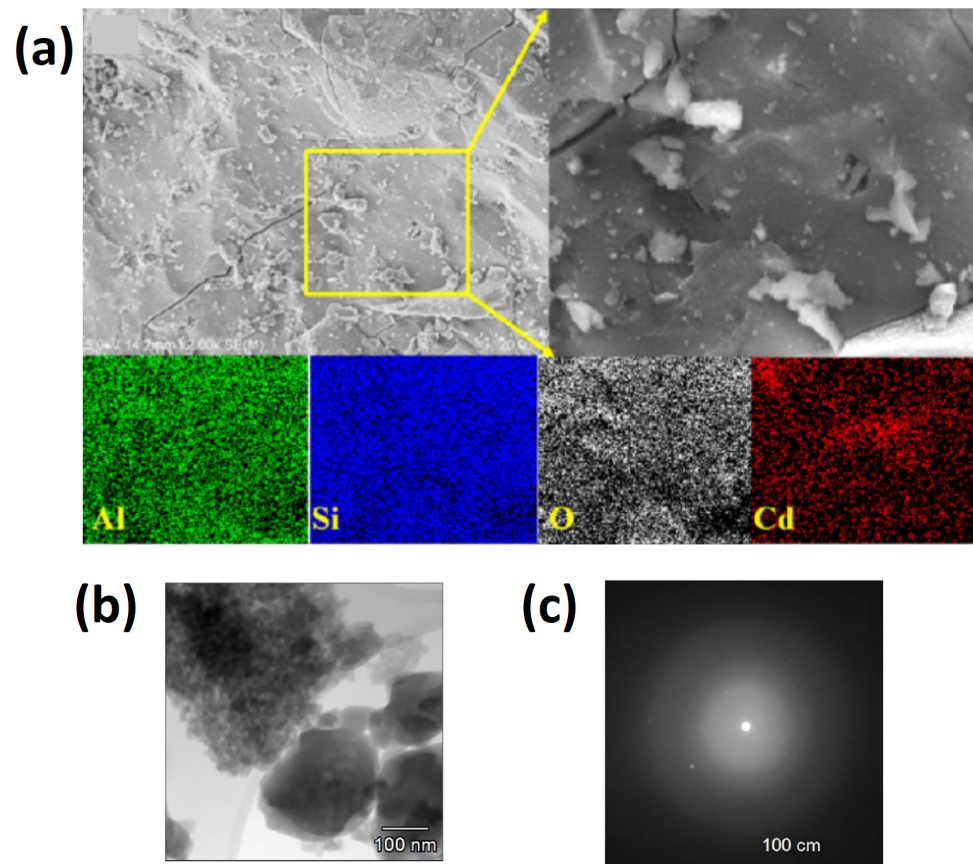


**Figure 3.** (a) SEM micrograph and elemental mapping of the geopolymers with immobilized Cd. (copyrighted, from [117]). (b) TEM micrograph of the metakaolin-based geopolymer and (c) the electron diffraction showing evidence of crystallinity (copyrighted, from [118] (CC BY 4.0)).

The pore structure is identified using gravimetric and absorption tests, e.g., MIP and BET, and the chemical structure is usually identified via spectroscopic analysis, e.g., XRF, Raman, FTIR, and NMR [112]. The most simple and versatile technique that can be employed for this purpose is Fourier-transform infrared (FTIR) spectroscopy analysis, which is widely used to identify the chemical structure and the changes that occur in it, in a qualitative way, by identifying the function groups and the shifts that occur in them. Typical geopolymer structure is confirmed by detecting the characteristics peaks of OH and M-O, where M is the metal, i.e., Si and/or Al. Figure 4 shows the results of the FTIR and Raman spectroscopy analysis for geopolymers prepared from chemicals (Figure 4a,b) and MK geopolymers with different prefabricated foam ratios (Figure 4c) [100,110]. FTIR spectra show the stretching vibration (near  $3500\text{ cm}^{-1}$ ) and bending vibration (near  $1650\text{ cm}^{-1}$ ) of the OH group. The characteristic M-O peaks appear near  $1050\text{--}1020\text{ cm}^{-1}$  and  $450\text{--}400\text{ cm}^{-1}$  represents the internal stretching vibration of the  $\text{SiO}_2$  tetrahedral and the bending of Si-O-Al. The shift of the peaks between the base material and the geopolymers can give insights into the inclusion of the Al in the Si tetrahedrons and the dissolution of the base material (Figure 4c). In addition, FTIR can clarify the changes in the geopolymers' composite structure in a comparative way, wherein the relative changes in the peak position and magnitude give indications on the changes that occur in the structure (Figure 4a). Raman spectroscopy can also be used in identifying the changes that occur in the crystalline inclusion within the geopolymers matrix. Figure 4b shows the characteristic peak for geopolymers at  $500\text{ cm}^{-1}$  and the changes in the crystalline layer houble hydroxide (LDH) due to its inclusion in geopolymers [110].

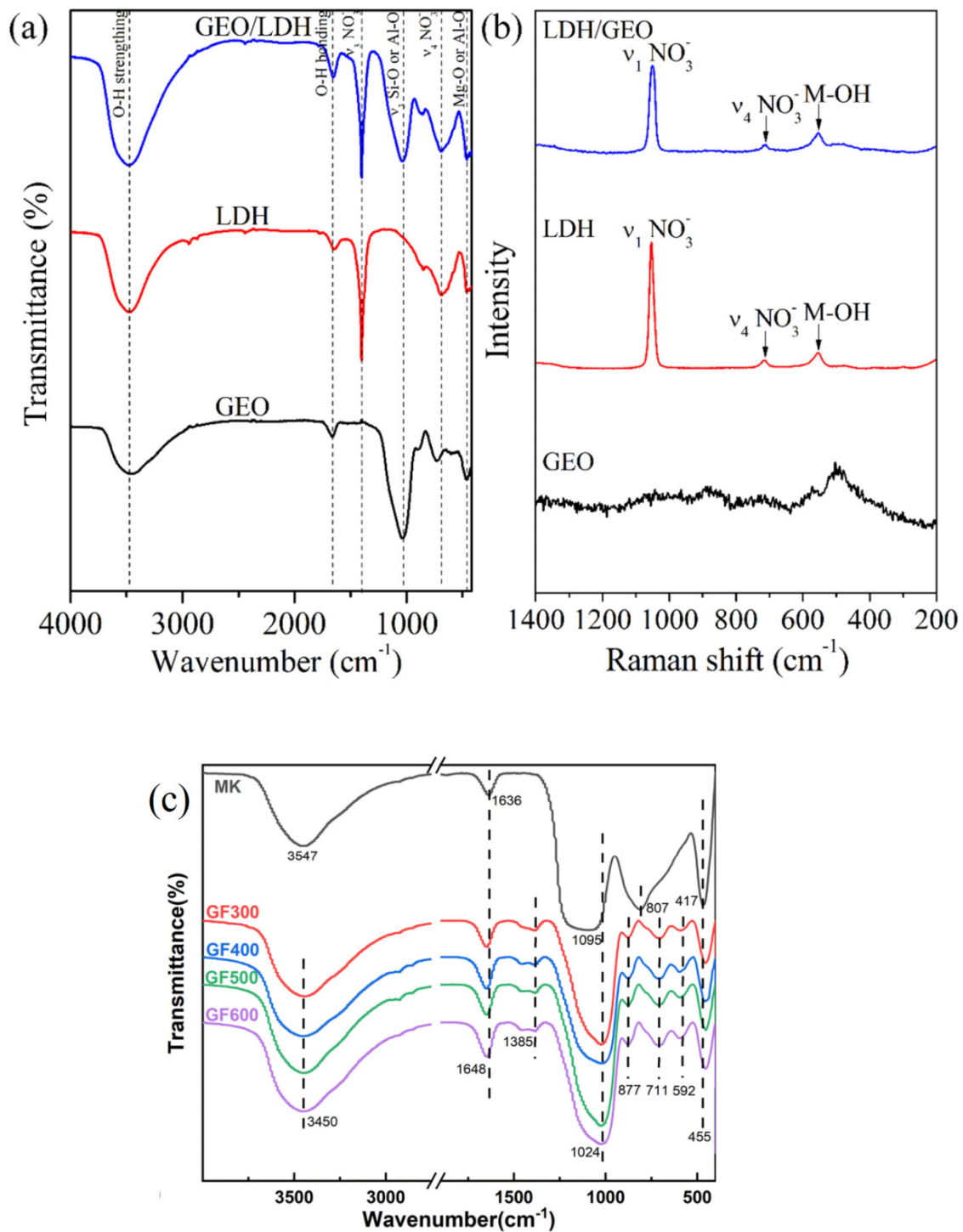


**Figure 4.** Geopolymer characterization using FTIR and Raman spectroscopy. (a,b) FTIR and Raman characterization for geopolymers prepared from chemicals and its modification with LDH (copyrighted, from [110]). (c) FTIR spectra for MK and geopolymers with prefabricated foam (copyrighted, from [100]).

To check if the prepared geopolymer contain any crystalline phases, either due to the incomplete dissolution of the crystalline base material or due to composite formation, XRD is considered a powerful tool. In general, the XRD pattern of amorphous silicate-based materials shows a diffuse hump that extends over the range 15–35°, and the inclusion of crystalline phases in these materials appears as characteristic Bragg peaks superimposed

on the hump [119]. Figure 5 presents the XRD results for geopolymers prepared from different sources and their composites [100,110,120]. The characteristic geopolymer diffuse hump reaches its peak near the quartz characteristic peak ( $\approx 27^\circ$ ) (Figure 5a–d). For geopolymers prepared from crystalline-based materials, the shift of the hump peak to higher  $2\theta$  values indicates the complete dissolution of the base materials. The characterization of geopolymers composites using XRD gives information on the inclusion of the crystalline phases within the geopolymers matrix and their crystallographic structure. Figure 5a,c shows the inclusion of LDH and sewage sludge ash (SSA) in geopolymers. The comparison between the geopolymer without SSA (Figure 5c) and with 30% SSA (Figure 5d) revealed that the crystalline waste, i.e., SSA, transformed to an amorphous structure during its reaction with the alkali solution [120]. That work concluded that the Cs leachability from the geopolymer matrix is improved over that of the OPC due to the following mechanisms [120]: (1) Cs is librated during the transformation of the crystalline SSA into amorphous structure; (2) the librated Cs is sorbed into the geopolymer matrix.

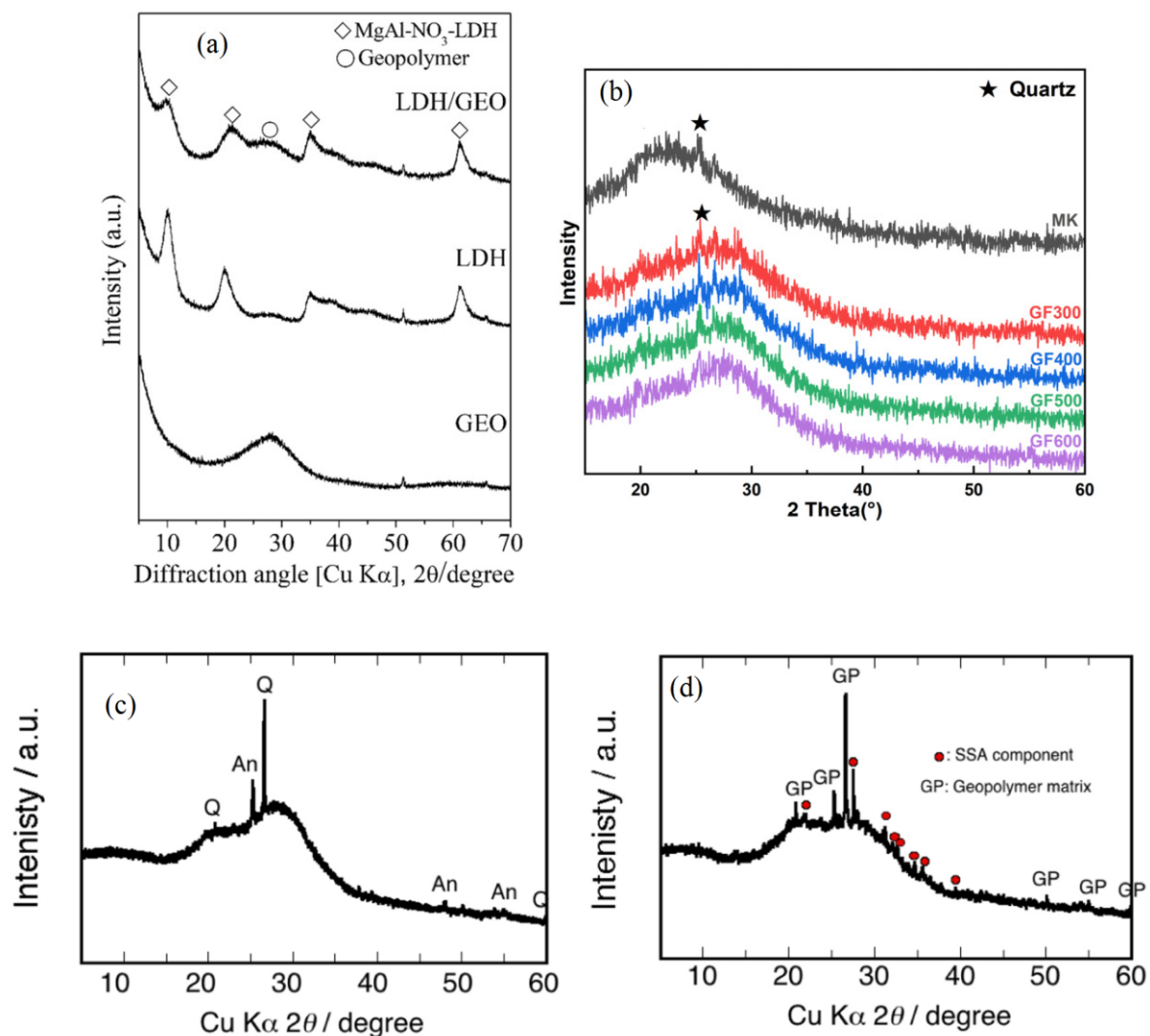


**Figure 5.** Geopolymer characterization using XRD (a) geopolymers prepared from chemicals (GEO), layer double hydroxide (LDH) and LDH—geopolymers composite (LDH/GEO) (Copyrighted, from [110]), (b) MK and geopolymers prepared with different inclusions of pre-fabricated foam (copyrighted, from [100]), (c) MK Geopolymer (copyrighted, from [120]) (d) MK—geopolymers with 30% sewage sludge ash (SSA) (copyrighted from [120]).

### 3. Geopolymers as Sorbents/Ion Exchangers for Radio-Contaminant Removal

Recent advancements in testing geopolymers for their potential applications in contaminant removal covered a wide spectrum of organic, inorganic, and biological contaminants, e.g., heavy metals, dyes, ammonium, sulfates, and microorganisms, etc. [75,77–79]. These efforts were motivated by the chemical and mechanical stability and the low energy and material footprints of these materials. In addition, the structure of the alumina silicate gel resembles the low and intermediate Si zeolites, which have a good electrostatic field that supports its application in the sorption of polar contaminants [95]. Subsequently, this class of material attracted workers in the field of radioactive waste treatment to test it.

Sorption/ion-exchange techniques are applied in nuclear reactors to control the system chemistry, minimize corrosion or degradation of system components, remove radioactive contaminants, and to clean and decontaminate aqueous streams during the operation of the power plant. Thus, this technique is used to decontaminate the primary coolant, primary effluents, wet storage waters, etc. [121]. In addition, it is employed in the treatment of liquid radioactive wastes generated from research centers, radioisotope production laboratories, uranium mining, and decommissioning activities of nuclear/radioactive facilities. Cs, Sr, Co, and Eu are used widely to test the performance of the cationic sorbents/exchangers for their potential applications in radioactive waste treatment; these elements are selected as models for alkali, alkaline earth, transition, and rare earth elements. In addition, Se, As, and I are used to assess the performance of anionic sorbents/exchangers.

#### 3.1. Types of Studied Geopolymers

The development of geopolymer technology revealed promising applications of geopolymers in the removal of radio-contaminants from aqueous waste streams by means of sorption/ion exchange. Of the many types of geopolymers, MK- and FA-based geopolymers were employed [20–28] since geopolymers were first introduced. The emergence of other types of base materials, e.g., slag and silica fume, has inspired researchers to use blended base materials instead of a single base material. In several studies, the successful testing of geopolymers formulated from blending different types of base materials were reported [20,24,25]. Lei et al. [24] fabricated MK/slag-based zeolite microsphere geopolymers to be used in the removal of  $\text{Cs}^+$  and  $\text{Sr}^{2+}$  from radioactively contaminated wastewater, and their findings revealed maximum adsorption capacities in batch sorption experiments equal to 103.74 and 54.90 mg/g, respectively. Earlier, Lee et al. [25] reported successful  $\text{Cs}^+$  adsorption onto a hybrid mesoporous geopolymer containing zeolites formulated from FA and slag. This hybrid geopolymer was able to remove more than 90% of  $\text{Cs}^+$ , and the maximum sorption capacity recorded was higher than most other materials including ceiling tiles, walnut shell, and chabazite pellets. The retention of  $\text{Cs}^+$  by geopolymers is benchmarked against ordinary Portland cement (OPC) and frequently shows higher retention compared to OPC. For instance, Jang et al. [22] reported higher Cs adsorption capacity for a FA-slag-based geopolymer (29.87–35.23 mg/g) compared to cement (19.09 mg/g). This result was attributed to the presence of aluminosilicate gel and the C-S-H with a low Ca/Si ratio in the FA/slag-based geopolymer [22,122,123]. These phases contain active sites that boost Cs sorption. In particular, the C-S-H with a low Ca/Si ratio was reported to have increased de-protonated weak sites in the silanol group compared to that in the C-S-H with a high Ca/Si ratio, which favors Cs sorption [124]. In comparison with the studied OPC in that work, the slag-based geopolymer was reported to have C-S-H with a higher Ca/Si ratio [22]. It is remarkable in that work that geopolymers prepared from FA only had better removal performance in terms of adsorption capacity compared to that of FA-slag geopolymers, which was attributed to the effect of increasing the slag on the extent of aluminosilicate gel formation [22].

The incorporation of other materials can provide additional sorption sites, as adopted by Chen et al. [26]; their study showed the increased removal of radioactive iodide ( $\text{I}^-$ ) from wastewater when hexa-decyl-tri-methyl-ammonium (HDTMA)-incorporated MK geopolymers were used. Petlitckaia et al. [28] developed a hybrid material with functionalized

sorbent (potassium copper hexacyanoferrate,  $K_2CuFe(CN)_6$ ) grafted onto a lightweight MK geopolymer foam to selectively remove  $Cs^+$  from radioactive aqueous waste. Their findings revealed that the grafted geopolymer showed very high selectivity for  $Cs^+$  in the presence of other cations compared to the un-grafted geopolymer. Additional material grafted onto the geopolymer is also useful for the purpose of the co-immobilization of more than one type of radionuclide, as shown by Tian and Sasaki [109], wherein a composite of layered double hydroxide/geopolymer (LDH/GEO) was employed for the adsorption of  $Cs^+$  and  $SeO_4^{2-}$ .

Alkali cations ( $Na^+$ ,  $K^+$ ) originating from the hydroxide or silicate activator may affect the sorption performance of geopolymers with favorable radionuclide sorption by a Na-based geopolymer, as indicated by Lee et al. [25] and El-Naggar and Amin [27]. The retention of radionuclides by geopolymers is also affected by the Si/Al ratio, as well as the temperature. A decrease in the pore volume with increasing Si/Al ratio was reported to result in the lower retention of radionuclides [23], whereas the presence of crystalline phases, i.e., nepheline or pollucite, that were formed during the high-temperature treatment of the geopolymer were reported to improve the retention of the radionuclides [23]. In another paper, the calcination of the MK/SA geopolymer was reported to reduce its ability to remove Cs from its aqueous solution [125]. This reduced sorption capacity is explained by the effect of the calcination temperature on the Al- coordination in the geopolymer, wherein a part of the Al tetrahedrons were proven to be transformed to penta- and hexahedrons with the increasing temperature. Moreover, it was found that approximately 10% of the aluminum on the surface of the calcined geopolymer decreased compared to the un-calcinated one.

### 3.2. Testing Techniques

There are two widely employed methods to test the performance of sorbents/ion exchangers, which are batch and column tests, to simulate the practical conditions during the operation. Batch tests are used to study the effect of the variation in the sorbent mass to the contaminated liquid volume (m/V, g/L), and the contaminated solution characteristics, i.e., the initial contamination level ( $C_o$ , ppm), the acidity or alkalinity (pH), and temperature (T, °C), under static conditions on the radio-contaminant removal behavior. Based on the field of application, either removal or separation, different performance measures can be obtained that include percentage removal, distribution coefficient, sorbed amount, and sorption capacity ( $Q_o$ , mg/g). In particular, the latter can be used as a base of comparison between the performances of different materials. Batch tests can be run to investigate the unsteady state behavior of the sorption process, i.e., kinetics and the equilibrium behavior. On one hand, the kinetic investigations are conducted to determine the time to reach equilibrium and rate constant and to have insights into the controlling removal mechanism. On the other hand, equilibrium investigations are employed to determine the sorption capacity, have information about the nature of the energy sites, and determine the reaction thermodynamic parameters. Several kinetics and equilibrium models are used to analyze these experimental data, a summary of these models and their features are found elsewhere [95]. Geopolymers prepared from chemicals, MK, FA, MK/slag, and FA/BFS (as indicated above), were tested to check their feasibility to be used in the removal of radio-contaminants; the researchers focused their efforts on studying the batch sorption behavior toward Cs and Sr (cations) and Se and As (anions) in aqueous solutions. Moreover, geopolymer composites with LDH, potassium copper hexacyanoferrate ( $K_2CuFe(CN)_6$ ), hexa decyl-tri-methyl-ammonium bromide (HDTMA), and iron (Fe) were tested to remove Cs, Sr, Se, I, and As. Tables 2 and 3 list the main studied experimental conditions, the specific surface area (SSA) of the geopolymers, and the main findings of these studies [20–28,98,100,109,110].

**Table 2.** Feasibility assessment of the use of geopolymers for radio-contaminant removal from aqueous solutions.

Base Material	Studied Experimental Conditions				SSA, m <sup>2</sup> /g	Main Findings				Ref.
	Cont.	C <sub>0</sub> , ppm	T, °C	m/V, g/L		t <sub>eq</sub> , min	pH <sub>Opt</sub>	Capacity, mg/g	Comments	
Chemical	Cs	100	-	1	121	60	8	-	2 <sup>nd</sup> order kinetics Monolayer sorption	[110]
	SeO <sub>4</sub> <sup>2-</sup>	100	-			30	8	-		
F/perlite	Cs	50	24.85–49.85	10	-	60	8	4.28**	2 <sup>nd</sup> order kinetics	[99]
	Eu	50	24.85–49.85			60	4	1.45**		
MK	Cs	100–1000	24.85–59.85	10	18.72	-	-	74.95*	Spontaneous endothermic reaction	[27]
	Cs	20–1000	24.85	1	37.77	120	7	216.1*	2 <sup>nd</sup> order kinetics Monolayer sorption Spontaneous endothermic reaction Reused for 2 cycles	[100]
FA	Cs	85–150	RT	1	-	10	>7	281.74*	2 <sup>nd</sup> order kinetics Monolayer sorption	[98]
	Sr					60		169.07*		
	Cs	100	RT	1	215	10	7	92.63	2 <sup>nd</sup> order kinetics Low Si/Al ratio result in better sorption of Cs+	[23]
MK/Slag	Cs	1000	-	1	77.6	10	-	59.56**	2 <sup>nd</sup> order kinetics Mixture of fly ash and slag reduces the removal performance	[22]
	Sr	1000	-			30	-	54.52**		
	Cs	10–170	25	1.2	23.22	30	>4	103.74*	2 <sup>nd</sup> order kinetics Monolayer sorption Regeneration for 4 and 2 cycles for Cs and Sr, respectively without significant loss***	[24]
	Sr	10–170	25	1.23		60	>4	54.91*		
FA& BFS	Cs	1000	-	1	12.72	30	-	29.22**	2 <sup>nd</sup> order kinetics Mixture of fly ash and slag reduces the removal performance	[22]
	Sr	1000	-			30	-	44.64**		
	Cs	10–150	-	10	114.16	40	4	15.24*	Multilayer sorption	[25]

\* Langmuir mono sorption capacity. \*\* Highest sorbed amount from kinetic only. \*\*\* studied column.

**Table 3.** Feasibility assessment of the use of geopolymers composites for radio- contaminant removal from aqueous solutions.

Base Material	Studied Experimental Conditions				SSA, m <sup>2</sup> /g	Main Findings				Ref.
	Cont.	C <sub>0</sub> , ppm	T, °C	m/V, g/L		t <sub>eq</sub> , min	pH <sub>Opt</sub>	Capacity, mg/g	Comments	
Chemical/LDH	Cs	100	-	1	134.1	120	8	84.14	2 <sup>nd</sup> order kinetics Monolayer sorption	[110]
	SeO <sub>4</sub> <sup>2-</sup>	100	-			5	8	71.3		
MK/K <sub>2</sub> CuFe(CN) <sub>6</sub> ]	Cs	3–1000	RT	1		4–5	-	250–175***	The material is very selective for Cs.	[28]
MK/HDTMA	I	250	24.85	1	35	180	>7	36.1**	2 <sup>nd</sup> order kinetics Multilayer spontaneous and exothermic process	[26]
FA/Fe	Cs	100	RT	1	107.9	10	7	111.9*	2 <sup>nd</sup> order kinetics Cs <sup>+</sup> & Sr <sup>2+</sup> monolayer sorption AsO <sub>4</sub> is multilayer sorption.	[21]
	Sr	100				30	7	14.19*		
	AsO <sub>4</sub> <sup>2-</sup>	50				150	5	21.51*		
MK-FA	Cs	27	25	2		120–240	7–7.5	113.3	The adsorption of geopolymer on Sr <sup>2+</sup> , Co <sup>2+</sup> , and Cs <sup>+</sup> is mainly chemical adsorption.	[20]
	Sr	18						85.7		
	Co	12						58.8		

\* Langmuir mono sorption capacity. \*\* experimental. \*\*\* studied desorption.

Column tests are used to investigate the sorption dynamics, optimize the column parameters, i.e., bed depth, flow rate, and identify the breakthrough curve characteristics. The application of the column technique in studying the removal performance of the radio-contaminants using geopolymer was limitedly addressed [24]. Cs and Sr removal using a MK/slag geopolymer was tested in a fixed-bed column with bed depth equal to 0.5 and 1 cm at two flow rates equal to 1 and 4 mL/min [24]. The breakthrough curve characteristics for the highest bed-depth and slowest flow-rate experiments were as follows: (1) the breakthrough points were 12 and 3.3 h; (2) the saturation points were 26 and 18 h; (3) the column adsorption capacities were 121.1 and 58.73 mg/g, respectively [24]. A recent paper studied Cs removal using a MK/sodium lauryl sulfate (SLS) geopolymer cylinder with diameter and height equal 0.5 and 0.7 cm, respectively, under varying flow rate of 20–50 mL/s [126]. The maximum adsorption capacities were reported to be 10.3–13 mg/g. In addition, the reusability and regeneration ability of the ion-exchanger/sorbent is an important topic to be identified to ensure the economic feasibility of the materials and to reduce the environmental footprint by reducing the material requirements for the treatment process [95]. The reusability and regeneration studies are very limited for geopolymer sorbents/ion exchangers. From the presented data herein on geopolymer testing for applications in radio-contaminant removal, the following remarks can be drawn:

- In terms of the number of conducted batch experiments, these experiments can provide a basis for evaluating the performance of the studied geopolymers, whereas the column and reusability and regeneration studies are lacking;
- The studied batch experimental data covered a wide range of initial contaminant concentrations in the range (3–1000 ppm) tested mostly at room temperature, except in two papers [27,99], and the sorbent-mass-to-liquid-volume ratio was in the range 1–10 g/L;
- The sorption data follow the pseudo-second-order reaction model, which shows that the reaction has a chemisorption nature that involves electron-sharing between the contaminants and the sorbent;
- For most of the sorption equilibrium batch tests, it was found that the sorption occurs on sites of equal energy, i.e., monolayer sorption, with exceptions for Cs removal using (FA/BFS) geopolymers and I and  $\text{AsO}_4^{2-}$  removal by MK/HDTMA and Fa/Fe geopolymers, respectively;
- The conducted thermodynamic studies indicated that the reactions were mainly spontaneous and endothermic, except for the removal of I using MK/HDTMA geopolymers.

#### 4. Geopolymers for the Immobilization of Radioactive Wastes

Using a geopolymer as a containment matrix for the immobilization of radio-contaminants involves the mixing of radioactive waste with a reactive base material (such as MK, FA) and/or an activating solution containing alkali ( $\text{Na}^+$  or  $\text{K}^+$ ) hydroxides and silicates, then applying suitable curing conditions [127]. This process aims, as in the case of other immobilization matrices, to produce an acceptable wastefrom that can comply with the regulatory requirements on radionuclide retention, water ingression, and structural stability provision in near-surface disposal facilities. The immobilization is achieved by solidification, embedding, or encapsulation [31]. The first is usually used to describe the immobilization of liquid and liquid-like wastes, and it is achieved through the chemical incorporation of the waste components into the structure of a suitable matrix. The latter is achieved by physically surrounding the waste in the immobilization matrix [108]. Basically, the radionuclides leachability is used as a performance measure to quantify the retention safety function. It is affected by the characteristics of the containment matrix, the radionuclide being leached, and the leaching environment [128]. Compressive strength and permeability are used as performance measures to quantify the provision of structural stability and for the prevention of water ingression, respectively.

#### 4.1. MK Based Geopolymer

Geopolymers have been investigated for the containment of radionuclides in low- and intermediate-level wastes (LILW) [33,129] that usually contain long-lived radionuclides, such as  $^{137}\text{Cs}$ ,  $^{90}\text{Sr}$ ,  $^{226}\text{Ra}$ ,  $^{232}\text{Th}$ , and  $^{238}\text{U}$ . Among the many radionuclides, Cs and Sr have been expansively studied due to their unfavorable immobilization by conventional cement-based materials. As for removal applications, MK geopolymers are frequently investigated by numerous researchers for radioactive waste immobilization [47,49,57,130–136]. Examples of these investigations include the immobilization of solid wastes generated from the nuclear fuel cycle that encompasses operational and decommissioning wastes from operating and decommissioned nuclear reactors, respectively [33]. Operational wastes such as graphite containing  $^{14}\text{C}$  has been successfully conditioned using geopolymers to produce a wastefrom with acceptable compressive strength and structural stability [60]. Another study addressed the immobilization of fuel cladding in MK geopolymers [101]. Besides solid waste, organic liquid wastes generated from nuclear reactors, such as lubricating oil contaminated with  $^{60}\text{Co}$  and  $^{137}\text{Cs}$ , have also been conditioned using MK geopolymers [62]. Moreover, secondary wastes, which are generated from the treatment of primary wastes, e.g., exhausted filters and ion exchangers/sorbents, have been tested for their potential immobilization in MK geopolymers. As in the case of the Fukushima Daiichi Accident, the feasibility of immobilizing spent ion-exchange resins containing  $^{137}\text{Cs}$  and  $^{90}\text{Sr}$  that resulted from the treatment of contaminated cooling water in a MK geopolymer was investigated. The immobilization of Sr-loaded titanate ion-exchangers in a MK geopolymer has proven the potential of the geopolymer as confinement matrix for this exhausted ion exchanger [134]. Similar findings were observed by Kuenzel et al. [135] for the immobilization of zeolite clinoptilolite ion exchangers contaminated with Cs and Sr. Walkley et al. [56] also observed the immobilization of  $^{90}\text{Sr}$  in ion-exchange resins by using MK geopolymers. One of the primary challenges in the immobilization of radioactive waste is the high sulfate content in some waste streams. Ahn et al. [35], in their study, have proven the applicability of using a MK geopolymer in immobilizing a high-sulfate hybrid sludge from a Hydrazine Based Reductive Metal Ion Decontamination (HyBRID) process that contained Fe, Ni, Cr, and Co ions with increased waste loading up to 53.8 wt%.

#### 4.2. Other Geopolymers

Other than MK geopolymers, FA geopolymers have also been investigated for the immobilization of different radio-contaminants, such as  $\text{Cs}^+$  [104]. Slag-based geopolymers have also been investigated for the immobilization of radio-contaminants in many radioactive waste streams. The advantages of geopolymers not only lie in their favorable mechanical strength and radionuclides stabilization potential but also in their waste loading capacity. For instance, a geopolymer prepared from GGBFS was applied successfully in the immobilization of ion-exchange resins contaminated with  $\text{Cs}^+$  and  $\text{Sr}^{2+}$  with maximum solidified wet resin content of about 45 wt% [51].

Blended materials were tested for their potential application to enhance the radio-contaminant retention, waste loading capacity, and mechanical strength of an immobilization matrix. As an example, the findings of Lin et al. [50] indicated the superior performance of geopolymer compared to cement when a blended MK-slag-based geopolymer was used for the immobilization of reactor spent resins containing  $\text{Cs}^+$  and  $\text{Sr}^{2+}$  with a loading capacity of ion-exchange resins up to 12 wt% (wet base). Similar findings were reported by El-Naggar [109] for the immobilization of  $^{60}\text{Co}$  using blended slag-seeded Egyptian Sinai kaolin geopolymer. As in the case of the well-known Hanford Project in the USA, the performance of the BFS-MK DuraLith geopolymer was enhanced, e.g., improved workability, reduced hydration heat, and higher waste loading, by the addition of fly ash [61].

Frequently, additional materials are incorporated into a geopolymer's formulation to either increase its radionuclides immobilization performance or to provide selective containment. These materials provide structure that creates extra fixation sites for radionuclides [137] or phases that favor the attachment of ions [138]. Besides the containment of

radionuclides, they may contribute to the enhancement of the mechanical strength of the geopolymer [51]. Moreover, these materials can cause changes to the chemical state of the radionuclides that further affect the performance of the geopolymers. Yu et al. [45] mentioned that, in the presence of Mn, Co was transformed from divalent to trivalent in an oxidation environment.

#### 4.3. Effect of Alkali Activator and Thermal Treatment

In terms of material types, another consideration is the type of the used alkali activators. In many studies, Na-based geopolymers showed better performance than K-based geopolymers [49,132,134]. This preference was attributed to the hard and soft acids and bases (HSAB) principles, in which high-charge-density  $\text{Na}^+$  resulted in  $\text{Na}^+$  being the stronger Lewis acid that favored reaction with  $\text{Cs}^+$  [134]. The incorporation of radionuclides into the geopolymer framework occurs through several mechanisms. One of the important mechanisms involved the replacement of alkali ions ( $\text{Na}^+$  and/or  $\text{K}^+$ ) by the radionuclide [56,134] with preference towards a Na-based geopolymer compared to a K-based geopolymer [48]. This replacement can cause structural changes to the geopolymers.

Apart from the types of used materials, the radionuclide containment performance of geopolymers is also affected by the thermal treatment of the geopolymer's matrix. Generally, geopolymers are thermally stable in a wide range of temperatures up to approximately 800 °C [139]. By exceeding this point up to around 1100 °C, crystalline phases are formed; nepheline forms in Na-based geopolymers; leucite forms in K-based geopolymers, and pollucite forms in the presence of Cs [48]. These crystalline phases have been shown to immobilize this radionuclide. The investigation of MK-based geopolymers formulated from the Na-alkali activator for Sr immobilization at different temperatures revealed lower  $\text{Sr}^{2+}$  leaching in the presence of nepheline structures formed by calcination in comparison to the uncalcinated geopolymer [135]. Few publications, however, noted the formation of these crystalline phases at lower temperatures [46,48], and the crystalline phases formed at these temperatures demonstrated better performance than the ones produced at high temperature. For instance, pollucite obtained at lower temperature via alkali metal ions doping and optimizing the Na/Cs ratio demonstrated high Cs immobilization compared to pollucite formed by a high-temperature hydrothermal treatment [140].

As much as geopolymer applications can, in certain cases, lead to better mechanical strength and durability compared to Portland cement, its dry shrinkage is relatively higher and therefore prone to cracking. Additionally, the geopolymer has also been found to have low affinity for anions, such as  $\text{SeO}_4^{2-}$  and  $\text{Cr}_2\text{O}_7^{2-}$  [141], which eventually hinders its application in immobilizing waste streams containing these contaminants. In order to rectify these shortcomings, the optimization of the alkali activator and the use of additive material can provide successful solutions for this problem [58,110].

Even though the application of a geopolymer in the immobilization of radioactive waste still remains largely in research stage, nevertheless the actual implementation has been adopted by the Slovak Republic. The immobilization of intermediate-level waste containing  $^{137}\text{Cs}$  from nuclear power reactors (sludge, resin, liquid wastes, and their mixtures) in Slovakia and Czech Republic was successfully implemented using a proprietary MK-based geopolymer matrix called SIAL [142].

#### 4.4. Geopolymers Performance

As indicated above, the radioactive wasteform should be designed to comply with the regulatory requirements on its safety functions, so they should be durable and able to mitigate the impact of anticipated accidents that can occur during its life time. The durability of the wasteform is affected by the waste compositions, amount of free water content, and the presence of environmental stressors that subsequently affect the characteristics of the wasteform (i.e., porosity, density, thermal and radiation stability, compressive strength, leaching resistance, chemical attack resistance, and freeze and thaw) [57,112,113,143–148]. It should be noted that the durability of the geopolymer under chemical attack is very

much dependent on the calcium content in the base material. It was reported that the high-calcium-content base material, i.e., class F fly ash, will produce a geopolymer more vulnerable to sulfate attack and carbonation than that with low calcium content [148]. Several durability tests were developed to test the sustainability of the safety function of the wasteforms throughout their life cycle [31,112,145–147]. In this section, the testing techniques and the analysis of the leaching behavior and compressive strength of the geopolymer wasteforms are presented.

#### 4.4.1. Testing Techniques

During the design of the wasteforms, there are several options that can be considered for testing these forms to ensure their sustainable performance. These options include the selection of the testing procedure, the factors that affect the wasteform performance, and the optimization technique. Details of these factors are found elsewhere [33]. Geopolymer studies addressed the sustainable performance of these wasteforms by evaluating the effect of geopolymer formulation on the radionuclide retention and compressive strength. In addition, the effects of the leaching solution on the wasteform stability, in terms of radionuclide leachability, were investigated. The effect of the freeze–thaw cycles, irradiation, and water immersion on the leaching and the compressive strength were quantified. The following subsections present the results of these investigations for different geopolymer types.

#### 4.4.2. Leaching Behavior of Geopolymer Wasteforms

The high pH environment of the cement-based material favors the stabilization of lanthanides and actinides within the immobilization matrix, yet alkali and alkaline metal remain substantially soluble depending on the waste constituents and the presence of additives [33]. Subsequently, most of the geopolymer studies were directed at assessing the potential of these materials to immobilize different primary and secondary waste streams contaminated with Cs and Sr and, to a lesser extent, Co, as mentioned in the previous sections [35,45–49,53–55,57,58,62,76,106]. In addition, the stabilization of some anions was addressed [58]. Most of the studied geopolymer were MK-based, with few tests for other geopolymers.

Several types of leaching procedures were employed in this respect, including the standardized ANSI/ANS, TCLP, and ASTM. The duration of the leaching-test applications varied from very-short-duration tests, i.e., 5 days [51], to longer-duration tests, i.e., 42 days [47,49,57]. The obtained leaching parameters were also very variable, including Cumulative Leach Fractions (CLF,  $\text{cm}^{-1}$ ), Normalized Leach Fraction (NLF,  $\text{g}\cdot\text{m}^{-2}\cdot\text{d}^{-1}$ ), Leach Rate (LR,  $\text{cm}\cdot\text{d}^{-1}$ ), Leaching index (Li), and Inhabitation grade (I, %). Tables 4 and 5 list the compositions of the studied immobilization matrices and the performed leaching tests and their results for Mk-based and other geopolymers, respectively. Despite the reported values of the leaching index providing insights into the acceptability of the wasteform performance, the variability of the reported leaching measures and the conducted leaching procedures inhibit the determination of a suitable geopolymer formulation to immobilize certain type of radioactive wastes.

Over the years, the utilization of geopolymers as a containment matrix has gained lots of attention, especially due to their improved performance in terms of thermal stability (at high temperature and during freeze–thaw cycles), acid resistance, mechanical strength, and radionuclide containment performance [47]. Findings from the study carried out by Liu et al. [55] suggested that the immobilization performance of the blended FA/slag/MK-based geopolymer exceeded that of cement as shown by the higher cumulative fraction leaching rate of cement compared to that of the geopolymer. In addition, the findings of Jang et al. [144] for the FA/slag-based geopolymer also showed better Cs- and Sr-containing radioactive-waste-immobilization performance in comparison to Portland cement and therefore proposing the potential of these geopolymers as promising barrier materials to retard the migration of radio-contaminants.

Table 4. Containment performance for metakaolin and metakaolin-blend geopolymers.

Studied Immobilization Matrix				Matrix Leaching Studies and Results			Ref.	
Base Material	Activators	Radionuclides Simulant/Waste	Waste Loading, %	Leach Test	Leaching Measure	Findings		
MK	SiO <sub>2</sub> , NaOH, or KOH, or LiOH	CsOH·H <sub>2</sub> O	14–20	ANSI/ANS 16.1	Li = 8.93–12.66 <sup>a</sup> NLR = 2.51 × 10 <sup>-4</sup> gm <sup>-2</sup> /d	Cs effectively immobilized in pollucite at ≤1000 °C.	[46]	
	Na <sub>2</sub> SiO <sub>3</sub> , SiO <sub>2</sub> and NaOH		2–18		Li = 8.93–12.66 <sup>a</sup>			
	Silica sol gel and NaOH	Cs OH	6–30	ANSI/ANS-16.1	NLR = 1.14 × 10 <sup>-3</sup> gm <sup>-2</sup> /d	Hydrothermal treatment increases the performance and compressive strength.	[48]	
	Sol gel NaOH	CsNO <sub>3</sub>	3.52	Leaching for 42 d	CLR < 1%	The Na-based geopolymer showed a lower leaching rate than the K-based geopolymer.	[49]	
		Sr(NO <sub>3</sub> ) <sub>2</sub>	5.82		CLR < 1%			
	KOH		<sup>152</sup> Eu	-	Leaching for 24 d	I = 98.9%	The radionuclides were not leached in water, even after the fine pulverization of samples, but remained in the geopolymer matrices.	[53]
			<sup>134</sup> Cs	-		I = 97.7%		
			<sup>60</sup> Co	-		I = 99.0%		
			<sup>59</sup> Fe	-		I = 99.0%		
	Water glass & H <sub>2</sub> O 17.6	Zeolite-loaded Sr	29.4	Leaching for 42	CLF = 1.8 × 10 <sup>-3</sup> cm <sup>-1</sup>	Has better leaching resistance than those of cement in different leaching solutions	[57]	
NaOH, KOH, Fumed silica, DIW	Sulfate ions in sludge	0–40%	-	CFL < 1.0%	-	[35]		
Sodium silicate NaOH	Heavy metals (Th(IV), U(VI), Pb(II), Cd(II), Cu(II))	-	Leaching for 24 h	LC: Deionized water = 11% 1 M HCl = 8% 0.1 M NaCl = 4.6% 1.0 M NaCl = 3.4% 0.1 M NaOH = 5.7%	The MK-based geopolymer is very effective in the stabilization of heavy metal ions.	[132]		
Na silicate	Sr	-	TCLP	Leaching rate: Deionized water at 1200 °C = 5.82 × 10 <sup>-7</sup> gm <sup>-2</sup> /d Simulated seawater at 1200 °C = 4.64 × 10 <sup>-6</sup> gm <sup>-2</sup> /d	Low leaching is achieved at higher temperature (1200 °C) due to the immobilization of Sr in nepheline structures.	[134]		

Table 4. Cont.

Studied Immobilization Matrix				Matrix Leaching Studies and Results			Ref.
Base Material	Activators	Radionuclides Simulant/Waste	Waste Loading, %	Leach Test	Leaching Measure	Findings	
MK/MS	Water glass & NaOH	CoCl <sub>2</sub>	5.56	TCLP	LC = 0.20%	Has higher acid-leaching resistance compared to the MK geopolymer	[45]
MK/Hydrotalcite/SF	Sodium silicate NaOH	SeO <sub>3</sub> <sup>2-</sup> SeO <sub>4</sub> <sup>2-</sup>	2	TCLP	LC = 10% -	Na <sub>2</sub> SiO <sub>3</sub> -activated geopolymers have better leaching performance than those of NaOH-activated geopolymers.	[58]
FA/BFS/MK/Sand/SF	The waste and NaOH KOH	Re	-	TCLP	LC = 0.65 mg/L	-	[61]
MK/B	Sodium silicate NaOH	Oil contaminated by Co	15.5–25	ASTM C130A for 12 day	LR = 8.5 × 10 <sup>-5</sup> cm/day	Leaching rate complied with the Brazilian regulations	[62]

<sup>a</sup> after thermal treatment to 1000C. SF = silica fume.

Table 5. Containment performance for fly ash and fly ash blend geopolymers.

Studied Immobilization Matrix				Matrix Leaching Studies and Results			Ref.
Base Material	Activators	Radionuclides Simulant/Waste	Waste Loading, %	Leach Test	Leaching Measure	Findings	
FA	Sodium silicate and NaOH	CsNO <sub>3</sub>	1.46	Leaching for 42 d	CFL = ~9 × 10 <sup>-3</sup> cm <sup>-1</sup>	-	[47]
GGBFS/Wollastonite	NaOH	Cs* Sr*	32%	Leaching for 5 days	CFL = 0.152 cm <sup>-1</sup> CFL = 9.72 × 10 <sup>-4</sup> cm <sup>-1</sup>	-	[51]
B/wood ash	NaOH	Sr	-	Leaching for 28 Day	NLR = 10 <sup>-6</sup> gm <sup>-2</sup> /d	The clay-based geopolymer shows better Sr immobilization than that of OPC.	[54]
FA/Slag/MK	-	Sr	-	-	CFL = 1.1 × 10 <sup>-3</sup> cm <sup>-1</sup>	FA/slag/MK has improved immobilization performance over that of OPC.	[55]
FA	Sodium silicate and aOH	CsNO <sub>3</sub>	2	ANSI/ANS 16 for 40 days	Li = 8.7–10.7	-	[105]

\* ion-exchange resin purolite NRW-10 and purolite NRW-4004.4.3 compressive strength of geopolymer wasteforms.

The compressive strength of the wastefoms is another key parameter that must meet the minimum criteria set by various regulatory bodies. The U.S. Nuclear Regulatory Commission (NRC) recommends a mean compressive strength of at least 500 psi (3.45 MPa) for wastefom specimens cured for a minimum of 28 days (ASTM C39/C39M-01). According to the standard GB 14569.1-2011 set by the National Standards of the People's Republic of China, which regulates the performance requirements for solidified wastefoms of low- and intermediate-level radioactive wastes, the compressive strength of the solidified sample should not be less than 7 MPa. Meanwhile, a minimum compressive strength of 4.9 MPa for low- and intermediate-level radioactive cementitious wastefoms are set by the Russian Federation (GOST R 51883–2002). Table 6 shows that the compressive strength of the geopolymer wastefoms reported in this review not only met the minimum criteria specified in the standards but also most of them exceeded the criteria by multiple folds.

**Table 6.** The compressive strength of the geopolymer wastefoms reported in the literature.

Geopolymer	Curing Conditions		Type of Simulant/Waste	Waste Loading (wt%)	$\sigma$ (MPa)	Ref.
	Temp. (°C)	Duration (Day)				
MK	25	7	Ba-loaded sludge waste	40.0	49.6	[35]
	60	2	Cs(OH) solution	47.7	65.8	[46]
	25	28	Sr-loaded zeolite	29.4	37.6	[57]
	25	28	Na <sub>2</sub> SeO <sub>3</sub> powder	2.45	30.0	[58]
	20	30	Nuclear graphite	10.0	22.0	[60]
	RT	28	Co-loaded bentonite	15.5–25	9.5 ± 0.9	[62]
Clay-based	RT	28	Sr-loaded wood ash	57.0	12.7	[54]
BFS	RT	28	Cs,Sr-loaded ion-exchange resins	5–45	10.2–22	[51]
FA/SF	60	28	<sup>133</sup> Cs <sup>+</sup> solution	2.0	57.2	[47]
MK/BFS	RT	28	Cs,Sr-loaded ion-exchange resins	12.0	13.6	[50]
	25	28	Sr(NO <sub>3</sub> ) <sub>2</sub> powder	9.0	24.5	[55]
FA/slag/Mk	RT	28	Re-loaded waste solution	26.8	57.5–121.7	[61]

The compressive strength of a wastefom can be affected by the chemical and physical properties, as well as the proportions of the radioactive wastes. Table 6 shows that the geopolymer wastefoms produced from liquid wastes [46,47,61] have higher compressive strength than the others. This better performance of liquid waste solidification is attributed to the ease of liquid-waste incorporation into the geopolymer slurries to form homogenous wastefoms after setting. In contrast, the insoluble solid wastes are encapsulated in the geopolymer slurries to form heterogeneous wastefoms. For example, it can be seen that the geopolymer wastefoms produced from spent ion-exchange resins [50,51] have relatively low compressive strength. The insoluble ion-exchange resins have weak contact with the geopolymer matrix, which, when under load, can easily lead to waste–matrix debonding, thus weakening the strength of the wastefoms.

The effect of the waste loading on the compressive strength of wastefoms was briefly investigated in the studies of Ahn et al. [35], Lin et al. [50], Lee et al. [51], and Liu et al. [55]. As for a comparison, the results from these studies are replotted with correlation coefficient values ( $R^2$ ) in Figure 6. In general, the waste loading influences the compressive strength of the wastefoms inversely. For example, strong and intermediate negative correlations are shown in the geopolymer wastefoms produced with spent ion-exchange resins [50,51] and Sr(NO<sub>3</sub>)<sub>2</sub> powder [55]. However, a weak correlation is shown in the geopolymer wastefoms with sludge waste, wherein the compressive strength initially decreased but increased at waste loading of 30 wt% and 40 wt%. [35]. This behavior was attributed, according to Ahn et al. [35], to the effect of the increased sludge waste loading on the

H<sub>2</sub>O/Al ratio in the geopolymer matrix, which led to a recovery of the compressive strength.

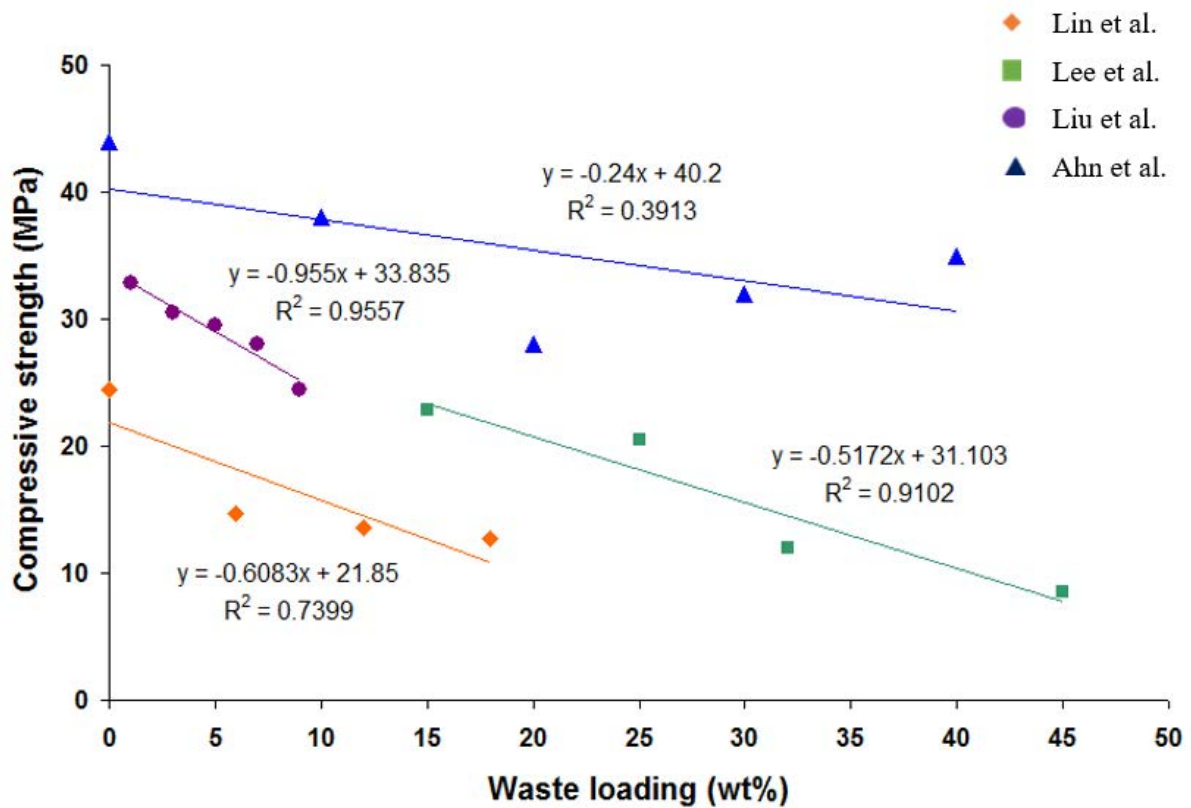


Figure 6. Compressive strength correlations with waste loading [35,50,51,55].

As for the type of binder matrix, there are no significant relationships between the geopolymer raw materials and wasteforms' compressive strength that can be observed in Table 6. However, Li et al. [47], Lee et al. [51], and Xu et al. [57], in their studies, have compared the compressive strength of geopolymer wasteforms with cement wasteforms. These studies found that, under the same conditions, wasteforms produced using geopolymers have significantly higher compressive strength than cement, as shown in Figure 7.

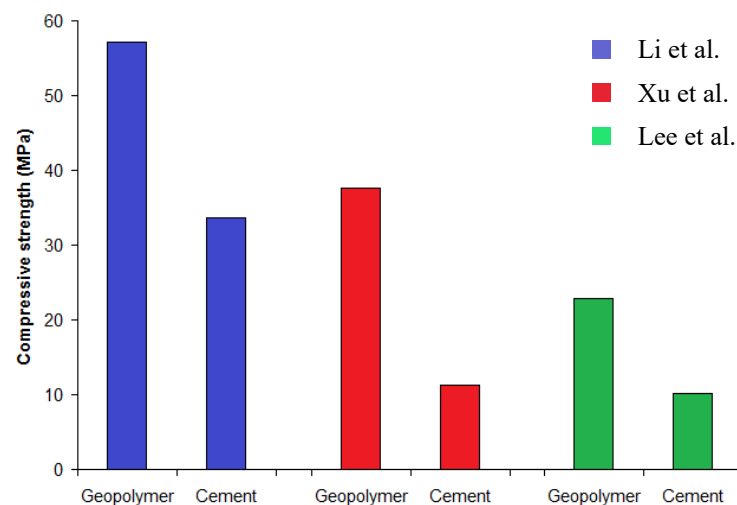


Figure 7. Compressive strength of geopolymer and cement wasteforms [47,51,57].

Besides being used as the basic criterion for solidified radioactive wasteforms, the compressive strength of a wasteform after calcination or freeze–thaw cycles are often used

to assess its stability and sustainable performance. Li et al. [47] reported that their studied geopolymer matrix maintained an adequate compressive strength after calcination at 1000 °C. In comparison, the compressive strength of their OPC matrix was reduced to just 5 MPa, as shown in Table 7. Similarly, Xu et al. [57] reported that effect of the temperature on the compressive strength in OPC is more significant than that in the geopolymer. It should be noted that the study of such a very-high-temperature effect is not required for low- and intermediate-level wastes that are not associated with heat generation and is not required for scenarios that do not include volcanic eruptions. These studies also showed that the losses of compressive strength due to freeze–thaw cycles ranged from 3.5 to 10.5%, with higher losses observed for cement wastefoms ranging from 14.7 to 18.2%, as shown in Table 8. Both studies concluded that geopolymer wastefoms are superior to cement wastefoms in thermal and freeze–thaw stability.

**Table 7.** Compressive strength of the geopolymer/cement wastefoms after thermal exposure.

Wastefoms	Compressive Strength (MPa)					Loss (%) after 1000 °C Calcination	Ref.
	Initial	400 °C	600 °C	800 °C	1000 °C		
Geopolymer	57	52	45	38	30	47.4	[47]
OPC	34	22	15	9	5	85.3	
Geopolymer	38	-	34	28	27	28.9	[57]
OPC	11	-	Cracked	Cracked	Cracked	100	

**Table 8.** Compressive strength of the geopolymer/cement wastefoms after freeze–thaw cycles test.

Wastefoms	Compressive Strength (MPa)		Loss (%)	Ref.
	Before Freeze–Thaw Test	After Freeze–Thaw Test		
Geopolymer	57	55	3.5	[47]
OPC	34	29	14.7	
Geopolymer	38	34	10.5	[57]
OPC	11	9	18.2	

## 5. Perspectives on the Sustainability of Geopolymers

The sustainability of any practice is based on its environmental impacts, economical performance, and social acceptance. Ensuring acceptable impacts and performance will enhance the social acceptance of that practice. As indicated in the introduction, the reduced environmental impacts of geopolymers compared to conventional cements and the use of industrial wastes as base materials for geopolymer fabrication boosted their applications as civil engineering materials. The sustainability assessments of the geopolymer concrete prepared from industrial wastes were addressed by identifying the factors that affect their compressive strength as a performance and durability measure [149–151]. In this respect, the effect of the preparation conditions of the geopolymer concrete on its compressive strength as a durability measure was assessed [149]. The results of that study revealed that the compressive strength of the geopolymer concrete prepared with a high content of calcium fly ash increased with increases in the molarity of the sodium activator, the activator-to-binder ratio, and the curing temperature, while it decreased with the increase in coarse aggregate content. In another study, the effect of the incorporation of corncob ash in a GGBFS-based geopolymer on compressive strength was assessed [150]. The study concluded that the environmental impacts, in terms of the transport impact, global warming potential, global temperature potential, embodied energy, sustainability index, and economic index of the studied geopolymer are less than that of conventional concrete.

The use of industrial waste as base material in the preparation of a geopolymer matrix for the immobilization of hazardous wastes were stated to reduce the greenhouse gas emis-

sions, energy requirements, and disposal costs of industrial wastes [86]. The study reported that the annual hazardous waste generation in India is 9.44 million tons, which requires 0.899 million tons of cement to stabilize. The use of an optimized geopolymer for different hazardous wastes was recommended to reduce the conventional cement requirements.

In Sections 3 and 4, the performance measures of different geopolymer materials were presented; these measures provide indicators on the potential sustainability of these materials in radioactive waste management. In addition, the limited large-scale industrial applications of these materials in the immobilization of radioactive wastes, i.e., SIAL, are providing additional measures of the potential sustainability of these materials. Nevertheless, the limited practical applications either in using geopolymers as sorbent or as immobilization matrices are not enough to generate a track record that enable the workers in this field to design specified durability tests that are based on geopolymer characteristics and performance. Additionally, the determinations of the sustainability indices for these applications are lacking. Moreover, the planning for radioactive waste management should be conducted in an integrated way that encompass the entire life cycle of the management practice. In this respect, life-cycle assessment for geopolymers in this field is also lacking.

## 6. Conclusions

Over the years, geopolymers have gained much attention in different fields, including radioactive waste management. The scientific efforts were focused on assessing the potential applications of these materials, as removal agents for radio-contaminants from liquid waste, and as immobilization matrices for different radioactive waste streams. This trend was supported by the need to reduce the material footprints in radioactive-waste-management activities and the promising performance of geopolymers in the water-and-wastewater-management field. Based on the literature reviewed in this work, the following gaps are identified in the sustainable performance of geopolymers in radioactive waste management:

- The application of a geopolymer in the pre-treatment of aqueous radioactive waste effluent was not addressed. This application is supported by the chemical stability of these materials in slightly acidic and alkaline solutions and its high buffering capacity, which allow an acceptable pH regulation performance.
- Geopolymer applications in membrane separation were not addressed in radioactive waste management. These applications are supported by the mechanical stability of these materials that are preserved even for porous geopolymers. This allows the application of geopolymer as a substrate or active layer in the membrane. Moreover, advanced trends in the literature were directed to assess this potential application in water and wastewater treatment and have provided knowledge that can be transferred to the radioactive-waste-management field.
- The ability of the amorphous geopolymer matrix to entrap metals and oxides can be used as a basis to test these materials for their potential application in photocatalytic degradation. This application, if proven, can be very useful to treat aqueous radioactive wastes that contain organic decontamination residues.
- As mentioned here, numerous batch studies were dictated to assess the promising application of geopolymers in radio-contaminant removal. These studies covered several types of geopolymer base materials, either single or blends, and targeted the removal of cations and anions of concern. Only a few studies have addressed the column operation and the reusability and regeneration ability of these materials, and there is still a need to investigate these aspects in depth and to have a clear understanding of the factors that affect them.
- The durability tests and standards were developed based on the long-term track record of the vulnerable characteristics of Portland cements. Despite geopolymers have been applied in certain countries for the immobilization of radioactive wastes, there is as yet no similar record to allow the adaptation of specific durability tests and standards for geopolymers.

- The life-cycle assessments for geopolymers used in radioactive waste management either as sorbent or as an immobilization matrix are lacking in the literature.

Even though most of the studies have yet to be implemented for actual application, they nevertheless serve as invaluable input for the further development of geopolymers in the field of radioactive waste management.

**Author Contributions:** Conceptualization, E.P., T.F.C. and R.O.A.R.; Resources, all the authors. All authors have read and agreed to the published version of the manuscript.

**Funding:** This research received no external funding.

**Institutional Review Board Statement:** Not applicable.

**Informed Consent Statement:** Not applicable.

**Data Availability Statement:** Not applicable.

**Acknowledgments:** The authors acknowledge the comments by anonymous reviewers, which helped to improve the review.

**Conflicts of Interest:** The authors declare no conflict of interest.

## References

1. Kim, H.J.; Kim, J.S.; Kim, K.P.; Kwon, J.H.; Kim, J.C.; Jeong, J.Y.; Kim, Y.K. Radiological impact assessment of radioactive effluents emitted from nuclear power plants in Korea and China under normal operation. *Prog. Nucl. Energy* **2022**, *153*, 104464. [CrossRef]
2. Abdel Rahman, R.O.; Kozak, M.W.; Hung, Y.-T. Radioactive pollution and control. In *Handbook of Environment and Waste Management*; Hung, Y.-T., Wang, L.K., Shamma, N.K., Eds.; World Scientific Publishing Co.: Singapore, 2014; pp. 949–1027. [CrossRef]
3. Ministry of Foreign Affairs, Report on the Discharge Record and the Seawater Monitoring Results at Fukushima Daiichi Nuclear Power Station during January, Information (18:00), March 1, 2022. Available online: <https://www.meti.go.jp/english/earthquake/nuclear/decommissioning/pdf/sd202203.pdf> (accessed on 2 January 2023).
4. IAEA. *Status and Trends in Spent Fuel and Radioactive Waste Management, Nuclear Energy Series, NW-T-1.14*; International Atomic Energy Agency: Vienna, Austria, 2022.
5. Gasser, M.S.; Kadry, H.F.; Helal, A.S.; Abdel Rahman, R.O. Optimization and modeling of uranium recovery from acidic aqueous solutions using liquid membrane with Lix-622 as Phenolic-oxime carrier. *Chem. Eng. Res. Des.* **2022**, *180*, 25–37. [CrossRef]
6. Ansari, S.A.; Mohapatra, P.K. Hollow fibre supported liquid membranes for nuclear fuel cycle applications: A review. *Clean. Eng. Technol.* **2021**, *4*, 100138. [CrossRef]
7. Kim, K.W.; Shon, W.J.; Oh, M.K.; Yang, D.; Foster, R.I.; Lee, K.Y. Evaluation of dynamic behavior of coagulation-flocculation using hydrous ferric oxide for removal of radioactive nuclides in wastewater. *Nucl. Eng. Technol.* **2019**, *51*, 738–745. [CrossRef]
8. Zheng, Y.; Qiao, J.; Yuan, J.; Shen, J.; Wang, A.J.; Niu, L. Electrochemical removal of radioactive cesium from nuclear waste using the dendritic copper hexacyanoferrate/carbon nanotube hybrids. *Electrochim. Acta* **2017**, *257*, 172–180. [CrossRef]
9. Chen, R.; Tanaka, H.; Kawamoto, T.; Asai, M.; Fukushima, C.; Kurihara, M.; Watanabe, M.; Arisaka, M.; Nankawa, T. Preparation of a film of copper hexacyanoferrate nanoparticles for electrochemical removal of cesium from radioactive wastewater. *Electrochem. Commun.* **2012**, *25*, 23–25. [CrossRef]
10. Osmanlioglu, A.E. Decontamination of radioactive wastewater by two-staged chemical precipitation. *Nucl. Eng. Technol.* **2018**, *50*, 886–889. [CrossRef]
11. Su, T.; Han, Z.; Qu, Z.; Chen, Y.; Lin, X.; Zhu, S. Effective recycling of Co and Sr from Co/Sr-bearing wastewater via an integrated Fe coagulation and hematite precipitation approach. *Environ. Res.* **2020**, *187*, 109654. [CrossRef] [PubMed]
12. Garai, M.; Yavuz, C.T. Radioactive strontium removal from seawater by a MOF via two-step ion exchange. *Chem* **2019**, *5*, 750–752. [CrossRef]
13. Gasser, A.M.S.; El Sherif, E.; Mekhamer, H.S.; Abdel Rahman, R.O. Assessment of Cyanex 301 impregnated resin for its potential use to remove cobalt from aqueous solutions. *Environ. Res.* **2020**, *185*, 10940. [CrossRef]
14. Allahkarami, E.; Rezaei, B. Removal of cerium from different aqueous solutions using different adsorbents: A review. *Process Saf. Environ. Prot.* **2019**, *124*, 345–362. [CrossRef]
15. Luo, W.; Huang, Q.; Antwi, P.; Guo, B.; Sasaki, K. Synergistic effect of  $\text{ClO}_4^-$  and  $\text{Sr}^{2+}$  adsorption on alginate-encapsulated organo-montmorillonite beads: Implication for radionuclide immobilization. *J. Colloid Interface Sci.* **2020**, *560*, 338–348. [CrossRef] [PubMed]
16. Kim, J.; Lee, K.; Seo, B.K.; Hyun, J.H. Effective removal of radioactive cesium from contaminated water by synthesized composite adsorbent and its thermal treatment for enhanced storage stability. *Environ. Res.* **2020**, *191*, 110099. [CrossRef] [PubMed]

17. Alipour, D.; Keshtkar, A.R.; Moosavian, M.A. Adsorption of thorium(IV) from simulated radioactive solutions using anovel electrospun PVA/TiO<sub>2</sub>/Zno nanofiber adsorbent functionalized with mercapto groups: Study in single and multi-component systems. *Appl. Surf. Sci.* **2016**, *366*, 19–29. [[CrossRef](#)]
18. Hasan, M.N.; Shenashen, M.A.; Hasan, M.M.; Znad, H.; Awual, M.R. Assessing of cesium removal from wastewater using functionalized wood cellulosic adsorbent. *Chemosphere* **2020**, *270*, 128668. [[CrossRef](#)]
19. Iwagami, S.; Tsujimura, M.; Onda, Y.; Konuma, R.; Sato, Y.; Sakakibara, K.; Yoschenko, V. Dissolved <sup>137</sup>Cs concentrations in stream water and subsurface water in a forested headwater catchment after the Fukushima Dai-Ichi Nuclear Power Plant accident. *J. Hydrol.* **2019**, *573*, 688–696. [[CrossRef](#)]
20. Chen, Y.L.; Tong, Y.Y.; Pan, R.W.; Tang, J. The research on adsorption behaviors and mechanisms of geopolymers on Sr<sup>2+</sup>, CO<sup>2+</sup> and Cs<sup>+</sup>. *Adv. Mater. Res.* **2013**, *704*, 313–318. [[CrossRef](#)]
21. Tian, Q.; Sasaki, K. Application of fly ash-based geopolymer for removal of cesium, strontium and arsenate from aqueous solutions: Kinetic, equilibrium and mechanism analysis. *Water Sci. Technol.* **2019**, *79*, 2116–2125. [[CrossRef](#)]
22. Jang, J.G.; Park, S.M.; Lee, H.K. Cesium and strontium retentions governed by aluminosilicate gel in alkali-activated cements. *Materials* **2017**, *10*, 447. [[CrossRef](#)]
23. Tian, Q.; Nakama, S.; Sasaki, K. Immobilization of cesium in fly ash-silica fume based geopolymers with different Si/Al molar ratios. *Sci. Total Environ.* **2019**, *687*, 1127–1137. [[CrossRef](#)]
24. Lei, H.; Muhammad, Y.; Wang, K.; Yi, M.; He, C.; Wei, Y.; Fujita, T. Facile fabrication of metakaolin/slag-based zeolite microspheres (M/Szms) geopolymer for the efficient remediation of Cs<sup>+</sup> and Sr<sup>2+</sup> from aqueous media. *J. Hazard. Mater.* **2021**, *406*, 124292. [[CrossRef](#)] [[PubMed](#)]
25. Lee, N.K.; Khalid, H.R.; Lee, H.K. Adsorption characteristics of cesium onto mesoporous geopolymers containing nano-crystalline zeolites. *Micropor. Mesopor. Mater.* **2017**, *242*, 238–244. [[CrossRef](#)]
26. Chen, S.; Qi, Y.; Cossa, J.J.; Dos, S.I.D.S. Efficient Removal of radioactive iodide anions from simulated wastewater by HDTMA-geopolymer. *Prog. Nucl. Energy* **2019**, *117*, 103112. [[CrossRef](#)]
27. El-Naggar, M.R.; Amin, M. Impact of alkali cations on properties of metakaolin and metakaolin/slag geopolymers: Microstructures in relation to sorption of <sup>134</sup>Cs radionuclide. *J. Hazard. Mater.* **2018**, *344*, 913–924. [[CrossRef](#)] [[PubMed](#)]
28. Petlitchkaia, S.; Barr, Y.; Piallat, T.; Grauby, O.; Ferry, D.; Poulesquen, A. Functionalized geopolymer foams for cesium removal from liquid nuclear waste. *J. Clean. Prod.* **2020**, *269*, 122400. [[CrossRef](#)]
29. IAEA. *Treatment and Conditioning of Radioactive Organic Liquids*; IAEA-TECDOC-656; IAEA: Vienna, Austria, 1992.
30. IAEA. *Predisposal Management of Organic Radioactive Waste*; Technical Reports Series No. 427; IAEA: Vienna, Austria, 2004.
31. Abdel Rahman, R.O.; Rakhimov, R.Z.; Rakhimova, N.R.; Ojovan, M.I. *Cementitious Materials for Nuclear Waste Immobilization*; Wiley: New York, NY, USA, 2014.
32. Varlakov, A.; Zherebtsov, A. Innovative and conventional materials and designs of nuclear cementitious systems in radioactive-waste management. In *Sustainability of Life Cycle Management for Nuclear Cementation-Based Technologies*; Abdel Rahman, R.O., Ojovan, M.I., Eds.; Elsevier-Woodhead Publishing: Chichester, UK, 2021; pp. 297–338.
33. Abdel Rahman, R.O.; Ojovan, M.I. Toward sustainable cementitious radioactive waste forms: Immobilization of problematic operational wastes. *Sustainability* **2021**, *13*, 11992. [[CrossRef](#)]
34. Abdel Rahman, R.O.; Abdel Moamen, O.A.; El-Masry, E.H. Life cycle of polymer nanocomposites matrices in hazardous waste management. In *Handbook of Polymer and Ceramic Nanotechnology*; Hussain, C.M., Thomas, S., Eds.; Springer Nature: Cham, Switzerland, 2021; pp. 1603–1625. [[CrossRef](#)]
35. Ahn, J.; Kim, W.S.; Um, W. Development of metakaolin-based geopolymer for solidification of sulfate-rich hybrid sludge waste. *J. Nucl. Mater.* **2019**, *518*, 247–255. [[CrossRef](#)]
36. Orlova, A.I.; Ojovan, M.I. Ceramic mineral waste-forms for nuclear waste immobilization. *Materials* **2019**, *12*, 2638. [[CrossRef](#)]
37. Fereiduni, E.; Ghasemi, A.; Elbestawi, M. Characterization of composite powder feedstock from powder bed fusion additive manufacturing perspective. *Materials* **2019**, *12*, 3673. [[CrossRef](#)]
38. Harker, A.B. Tailored ceramics. In *Radioactive Waste Forms for the Future*; Lutze, W.R.E., Ed.; North-Holland: Amsterdam, The Netherlands, 1988; pp. 335–392.
39. Frolova, A.V.; Vinokurov, S.E.; Gromyak, I.N.; Danilov, S.S. Medium-temperature phosphate glass composite material as a matrix for the immobilization of high-level waste containing volatile radionuclides. *Energies* **2022**, *15*, 7506. [[CrossRef](#)]
40. Farid, O.M.; Ojovan, M.I.; Massoud, A.; Abdel Rahman, R.O. An assessment of initial leaching characteristics of alkali-borosilicate-glasses for nuclear waste immobilization. *Materials* **2019**, *12*, 1462. [[CrossRef](#)] [[PubMed](#)]
41. Lönartz, M.I.; Dohmen, L.; Lenting, C.; Trautmann, C.; Lang, M.; Geisler, T. The effect of heavy ion irradiation on the forward dissolution rate of borosilicate glasses studied in situ and real time by Fluid-Cell Raman Spectroscopy. *Materials* **2019**, *12*, 1480. [[CrossRef](#)] [[PubMed](#)]
42. Ojovan, M.I.; Lee, W.E.; Kalmykov, S.N. Immobilization of radioactive waste in cement. In *An Introduction to Nuclear Waste Immobilization*, 3rd ed.; Ojovan, M.I., Lee, W.E., Kalmykov, S.N., Eds.; Elsevier: Amsterdam, The Netherlands, 2019; pp. 271–303.
43. Isaacs, M.; Lange, S.; Deissmann, G.; Bosbach, D.; Milodowski, A.E.; Read, D. Retention of technetium-99 by grout and backfill cements: Implications for the safe disposal of radioactive waste. *Appl. Geochem.* **2020**, *116*, 104580. [[CrossRef](#)]
44. Bayoumi, T.A.; Saleh, H.M. Characterization of biological waste stabilized by cement during immersion in aqueous media to develop disposal strategies for phytomediated radioactive waste. *Prog. Nucl. Energy* **2018**, *107*, 83–89. [[CrossRef](#)]

45. Yu, Q.; Li, S.; Li, H.; Chai, X.; Bi, X.; Liu, J.; Ohnuki, T. Synthesis and characterization of Mn-slag based geopolymer for immobilization of Co. *J. Clean. Prod.* **2019**, *234*, 97–104. [[CrossRef](#)]
46. He, P.; Wang, R.; Fu, S.; Wang, M.; Cai, D.; Ma, G.; Wang, M.; Yuan, J.; Yang, Z.; Duan, X.; et al. Safe trapping of cesium into doping-enhanced pollucite structure by geopolymer precursor technique. *J. Hazard. Mater.* **2019**, *367*, 577–588. [[CrossRef](#)]
47. Li, Q.; Sun, Z.; Tao, D.; Xu, Y.; Li, P.; Cui, H.; Zhai, J. Immobilization of simulated radionuclide  $^{133}\text{Cs}^+$  by fly ash-based geopolymer. *Radiat. Phys. Chem.* **2013**, *262*, 325–331. [[CrossRef](#)]
48. Fu, S.; He, P.; Wang, M.; Cui, J.; Wang, M.; Duan, X.; Yang, Z.; Jia, D.; Zhou, Y. Hydrothermal synthesis of pollucite from metakaolin-based geopolymer for hazardous wastes storage. *J. Clean. Prod.* **2020**, *248*, 119240. [[CrossRef](#)]
49. He, P.; Cui, J.; Wang, M.; Fu, S.; Yang, H.; Sun, C.; Duan, X.; Yang, Z.; Jia, D.; Zhou, Y. Interplay between storage temperature, medium and leaching kinetics of hazardous wastes in metakaolin-based geopolymer. *J. Hazard. Mater.* **2020**, *384*, 121377. [[CrossRef](#)]
50. Lin, W.K.; Chen, H.Y.; Huang, C.P. Performance study of ion exchange resins solidification using metakaolin-based geopolymer binder. *Prog. Nucl. Energy* **2020**, *129*, 103508. [[CrossRef](#)]
51. Lee, W.H.; Cheng, T.W.; Ding, Y.C.; Lin, K.L.; Tsao, S.W.; Huang, C.P. Geopolymer technology for the solidification of simulated ion exchange resins with radionuclides. *J. Environ. Manag.* **2019**, *235*, 19–27. [[CrossRef](#)] [[PubMed](#)]
52. Williams, B.D.; Neeway, J.J.; Snyder, M.M.V.; Bowden, M.E.; Amonette, J.E.; Arey, B.W.; Pierce, E.M.; Brown, C.F.; Qafoku, N.P. Mineral assemblage transformation of a metakaolin-based waste form after geopolymer encapsulation. *J. Nucl. Mater.* **2016**, *473*, 320–332. [[CrossRef](#)]
53. Hanzlicek, T.; Steinerova, M.; Straka, P. Radioactive metal isotopes stabilized in a geopolymer matrix: Determination of a leaching extract by a radiotracer method. *J. Am. Ceram. Soc.* **2006**, *89*, 3541–3543. [[CrossRef](#)]
54. Chervonnyj, A.D.; Chervonnaya, N.A. Geopolymeric agent for immobilization of radioactive ashes from biomass burning. *Radiochemistry* **2003**, *45*, 182–188. [[CrossRef](#)]
55. Liu, X.; Ding, Y.; Lu, X. Immobilization of simulated radionuclide  $^{90}\text{Sr}$  by fly ash-slag-metakaolin-based geopolymer. *Nucl. Technol.* **2017**, *198*, 64–69. [[CrossRef](#)]
56. Walkley, B.; Ke, X.; Hussein, O.H.; Bernal, S.A.; Provis, J.L. Incorporation of strontium and calcium in geopolymer gels. *J. Hazard. Mater.* **2020**, *382*, 121015. [[CrossRef](#)] [[PubMed](#)]
57. Xu, Z.; Jiang, Z.; Wu, D.; Peng, X.; Xu, Y.; Li, N.; Qi, Y.; Li, P. Immobilization of strontium-loaded zeolite A by metakaolin-based geopolymer. *Ceram. Int.* **2017**, *43*, 4434–4439. [[CrossRef](#)]
58. Tian, Q.; Guo, B.; Sasaki, K. Immobilization mechanism of Se oxyanions in geopolymer: Effects of alkaline activators and calcined hydrotalcite additive. *J. Hazard. Mater.* **2020**, *387*, 121994. [[CrossRef](#)]
59. Cannes, C.; Rodrigues, D.; Barré, N.; Lambertin, D.; Delpéch, S. Reactivity of uranium in geopolymers, confinement matrices proposed to encapsulate MgZr Waste. *J. Nucl. Mater.* **2019**, *518*, 370–379. [[CrossRef](#)]
60. Girke, N.A.; Steinmetz, H.J.; Bukaemsky, A.; Bosbach, D.; Hermannand, E.; Griebel, I. Cementation of Nuclear Graphite using Geopolymers. In Proceedings of the NUWCEM 2011, Avignon, France, 11–14 October 2011.
61. Xu, H.; Gong, W.; Syltebo, L.; Lutze, W.; Pegg, I.L. Duralith geopolymer waste form for Hanford secondary waste: Correlating setting behavior to hydration heat evolution. *J. Hazard. Mater.* **2014**, *278*, 34–39. [[CrossRef](#)]
62. Cuccia, V.; Freire, C.B.; Ladeira, A.C.Q. Radwaste oil immobilization in geopolymer after non-destructive treatment. *Prog. Nucl. Energy* **2020**, *122*, 103246. [[CrossRef](#)]
63. Ren, B.; Zhao, Y.; Bai, H.; Kang, S.; Zhang, T.; Song, S. Eco-friendly geopolymer prepared from solid wastes: A critical review. *Chemosphere* **2021**, *267*, 128900. [[CrossRef](#)]
64. Sercombe, J.; Gwinner, B.; Tiffreau, C.; Simondi-Teisseire, B.; Adenot, F. Modelling of bituminized radioactive waste leaching. Part I: Constitutive equations. *J. Nucl. Mater.* **2006**, *349*, 96–106. [[CrossRef](#)]
65. Zakharova, K.P.; Masanov, O.L. Bituminization of liquid radioactive waste. Safety assessment and operational experience. *Atomic Energy* **2000**, *89*, 135–139. [[CrossRef](#)]
66. Ikladios, N.E.; Ghattasv, N.K.; Tawfik, M.E. Some Studies on the incorporation of simulate radioactive waste into polymer matrix. *Radioact. Waste Manag. Nucl. Fuel Cycle* **1993**, *17*, 119–137.
67. Özdemir, T.; Usanmaz, A. Monte Carlo simulations of radioactive waste embedded into polymer. *Rad. Phys. Chem.* **2009**, *78*, 800–805. [[CrossRef](#)]
68. Davidovits, J. *Geopolymer Chemistry and Applications*, 4th ed.; Geopolymer Institute: Saint-Quentin, France, 2015.
69. Zakka, W.P.I.; Lim, N.H.A.S.; Khun, M.C. A scientometric review of geopolymer concrete. *J. Clean. Prod.* **2021**, *280*, 124353. [[CrossRef](#)]
70. Wang, S.; Li, H.; Zou, S.; Zhang, G. Experimental research on afeasible rice husk/geopolymer foam building insulation material. *Energy Build.* **2020**, *226*, 110358. [[CrossRef](#)]
71. Jiang, C.; Wang, A.; Bao, X.; Ni, T.; Ling, J. A review on geopolymer in potential coating application: Materials, preparation and basic properties. *J. Build. Eng.* **2020**, *32*, 101734. [[CrossRef](#)]
72. Villalquirañ-Cacedo, M.A.; Mejía de Gutiérrez, R. Synthesis of ceramic materials from ecofriendly geopolymer precursors. *Mater. Lett.* **2018**, *230*, 300–304. [[CrossRef](#)]
73. Lahoti, M.; Tan, K.H.; Yang, E.H. A critical review of geopolymer properties for structural fire-resistance applications. *Constr. Build. Mater.* **2019**, *221*, 514–526. [[CrossRef](#)]

74. Zhang, Y.J.; Han, Z.C.; He, P.Y.; Chen, H. Geopolymer-based catalysts for cost-effective environmental governance: A review based on source control and end-of-pipe treatment. *J. Clean. Prod.* **2020**, *263*, 121556. [[CrossRef](#)]
75. Łach, M.; Mierzwiński, D.; Korniejewski, K.; Mikula, J.; Hebda, M. Geopolymers as a material suitable for immobilization of fly ash from municipal waste incineration plants. *J. Air Waste Manag. Assoc.* **2018**, *68*, 1190–1197. [[CrossRef](#)] [[PubMed](#)]
76. Tochetto, G.A.; Simão, L.; de Oliveira, D.; Hotza, D.; Immich, A.P.S. Porous geopolymers as dye adsorbents: Review and perspectives. *J. Clean. Prod.* **2022**, *374*, 133982. [[CrossRef](#)]
77. Freire, A.L.; José, H.J.; Moreira, R.D.F.P.M. Potential applications for geopolymers in carbon capture and storage. *Int. J. Greenh. Gas Control.* **2022**, *118*, 103687. [[CrossRef](#)]
78. Luhar, I.; Luhar, S.; Abdullah, M.M.A.B.; Razak, R.A.; Vizureanu, P.; Sandu, A.V.; Matasar, P.D. A state-of-the-art review on innovative geopolymer composites designed for water and wastewater treatment. *Materials* **2021**, *14*, 7456. [[CrossRef](#)] [[PubMed](#)]
79. Sadiq, M.; Naveed, A.; Arif, M.; Hassan, S.; Afridi, S.; Asif, M.; Sultana, S.; Amin, N.; Younas, M.; Khan, M.N.; et al. Geopolymerization: A promising technique for membrane synthesis. *Mater. Res. Express* **2021**, *8*, 112002. [[CrossRef](#)]
80. Della Rocca, D.G.; Peralta, R.M.; Peralta, R.A.; Rodríguez-Castellón, E.; de Fatima Peralta Muniz Moreira, R. Adding value to aluminosilicate solid wastes to produce adsorbents, catalysts and filtration membranes for water and wastewater treatment. *J. Mater. Sci.* **2021**, *56*, 1039–1063. [[CrossRef](#)]
81. Novais, R.M.; Pullar, R.C.; Labrincha, J.A. Geopolymer foams: An overview of recent advancements. *Prog. Mater. Sci.* **2020**, *109*, 100621. [[CrossRef](#)]
82. Wu, Y.; Lu, B.; Bai, T.; Wang, H.; Du, F.; Zhang, Y.; Cai, L.; Jiang, C.; Wang, W. Geopolymer, green alkali activated cementitious material: Synthesis, applications and challenges. *Constr. Build. Mater.* **2019**, *224*, 930–949. [[CrossRef](#)]
83. Ji, Z.; Pei, Y. Bibliographic and visualized analysis of geopolymer research and its application in heavy metal immobilization: A review. *J. Environ. Manag.* **2019**, *231*, 256–267. [[CrossRef](#)] [[PubMed](#)]
84. El-eswed, B.I. Chemical evaluation of immobilization of wastes containing Pb, Cd, Cu and Zn in alkali-activated materials: A critical review. *J. Environ. Chem. Eng.* **2020**, *8*, 104194. [[CrossRef](#)]
85. Taki, K.; Mukherjee, S.; Patel, A.K.; Kumar, M. Reappraisal review on geopolymer: A new era of aluminosilicate binder for metal immobilization. *Environ. Nanotechnol. Monit. Manag.* **2020**, *14*, 100345. [[CrossRef](#)]
86. Singh, R.; Budarayavalasa, S. Solidification and stabilization of hazardous wastes using geopolymers as sustainable binders. *J. Mater. Cycles Waste Manag.* **2021**, *23*, 1699–1725. [[CrossRef](#)]
87. Tian, Q.; Bai, Y.; Pan, Y.; Chen, C.; Yao, S.; Sasaki, K.; Zhang, H. Application of geopolymer in stabilization/solidification of hazardous pollutants: A review. *Molecules* **2022**, *27*, 4570. [[CrossRef](#)] [[PubMed](#)]
88. Liang, K.; Wang, X.Q.; Chow, C.L.; Lau, D. A review of geopolymer and its adsorption capacity with molecular insights: A promising adsorbent of heavy metal ions. *J. Environ. Manag.* **2022**, *322*, 116066. [[CrossRef](#)]
89. Li, J.; Chen, L.; Wang, J. Solidification of radioactive wastes by cement-based materials. *Prog. Nucl. Energy* **2021**, *141*, 103957. [[CrossRef](#)]
90. Reeb, C.; Pierlot, C.; Davy, C.; Lambertin, D. Incorporation of organic liquids into geopolymer materials—A review of processing, properties and applications. *Ceram. Int.* **2021**, *47*, 7369–7385. [[CrossRef](#)]
91. Provis, J.L.; van Deventer, J.S.J. Geopolymerisation kinetics. 2. Reaction kinetic modelling. *Chem. Eng. Sci.* **2007**, *62*, 2318–2329. [[CrossRef](#)]
92. Luhar, I.; Luhar, S. A comprehensive review on fly ash-based geopolymer. *J. Compos. Sci.* **2022**, *6*, 219. [[CrossRef](#)]
93. Davidovits, J. *Geopolymer Chemistry and Applications*; Geopolymer Institute: Saint-Quentin, France, 2008.
94. Weng, L.; Sagoe-Crentsil, K. Dissolution processes, hydrolysis and condensation reactions during geopolymer synthesis: Part I—Low Si/Al ratio systems. *J. Mater. Sci.* **2007**, *42*, 2997–3006. [[CrossRef](#)]
95. Abdel Rahman, R.O.; El-Kamash, A.M.; Hung, Y.-T. Applications of nano-zeolite in wastewater treatment: An overview. *Water* **2022**, *14*, 137. [[CrossRef](#)]
96. Blackford, M.G.; Hanna, J.V.; Pike, K.J.; Vance, E.R.; Perera, D.S. Transmission electron microscopy and nuclear magnetic resonance studies of geopolymers for radioactive waste immobilization. *J. Am. Ceram. Soc.* **2007**, *90*, 1193–1199. [[CrossRef](#)]
97. Duxson, P.; Provis, J.L.; Lukey, G.C.; Mallicoate, S.W.; Kriven, W.M.; Van Deventer, J.S. Understanding the relationship between geopolymer composition, microstructure and mechanical properties. *Colloids Surf. A Physicochem. Eng. Asp.* **2005**, *269*, 47–58. [[CrossRef](#)]
98. Tian, Q.; Sasaki, K. Application of fly ash-based materials for stabilization/solidification of cesium and strontium. *Environ. Sci. Pollut. Res.* **2019**, *26*, 23542–23554. [[CrossRef](#)] [[PubMed](#)]
99. Youssef, M.A.; El-Naggar, M.R.; Ahmed, I.M.; Attallah, M.F. Batch kinetics of  $^{134}\text{Cs}$  and  $^{152+154}\text{Eu}$  radionuclides onto polycondensed feldspar and perlite based sorbents. *J. Hazard. Mater.* **2021**, *403*, 123945. [[CrossRef](#)]
100. Xiang, Y.; Hou, L.; Liu, J.; Li, J.; Lu, Z.; Niu, Y. Adsorption and enrichment of simulated  $^{137}\text{Cs}$  in geopolymer foams. *J. Environ. Chem. Eng.* **2021**, *9*, 105733. [[CrossRef](#)]
101. Rooses, A.; Steins, P.; Dannoux-Papin, A.; Lambertin, D.; Poulesquen, A.; Frizon, F. Encapsulation of Mg–Zr alloy in metakaolin-based geopolymer. *Appl. Clay Sci.* **2013**, *73*, 86–92. [[CrossRef](#)]
102. Leay, L.; Potts, A.; Donocli, T. Geopolymers from fly ash and their gamma irradiation. *Mater. Lett.* **2018**, *227*, 240–242. [[CrossRef](#)]
103. Lambertin, D.; Boher, C.; Dannoux-Papin, A.; Galliez, K.; Rooses, A.; Frizon, F. Influence of gamma ray irradiation on metakaolin based sodium geopolymer. *J. Nucl. Mater.* **2013**, *443*, 311–315. [[CrossRef](#)]

104. Chartier, D.; Sanchez-Canet, J.; Bessette, L.; Esnouf, S.; Renault, J.P. Influence of formulation parameters of cement based materials towards gas production under gamma irradiation. *J. Nucl. Mater.* **2018**, *511*, 183–190. [[CrossRef](#)]
105. Kumagai, Y.; Kimura, A.; Taguchi, M.; Nagaishi, R.; Yamagishi, I.; Kimura, T. Hydrogen production in gamma radiolysis of the mixture of mordenite and seawater. *J. Nucl. Sci. Technol.* **2013**, *50*, 130–138. [[CrossRef](#)]
106. Deng, N.; An, H.; Cui, H.; Pan, Y.; Wang, B.; Mao, L.; Zhai, J. Effects of gamma-ray irradiation on leaching of simulated  $^{133}\text{Cs}$ + radionuclides from geopolymer wasteforms. *J. Nucl. Mater.* **2015**, *459*, 270–275. [[CrossRef](#)]
107. Ojovan, M.I. Radioactive waste characterization and selection of processing technologies. In *Handbook of Advanced Radioactive Waste Conditioning Technologies*; Woodhead Publishing Limited Chichester: Chichester, UK, 2011; pp. 1–18.
108. Ojovan, M.I.; Lee, W.E. Introduction to immobilization. In *An Introduction to Nuclear Waste Immobilization*; Elsevier: Amsterdam, The Netherlands, 1989; pp. 1–8. ISBN 9780080444628.
109. El-Naggar, M.R. Applicability of alkali activated slag-seeded Egyptian Sinai kaolin for the immobilization of  $^{60}\text{Co}$  radionuclide. *J. Nucl. Mater.* **2014**, *447*, 15–21. [[CrossRef](#)]
110. Tian, Q.; Sasaki, K. A novel composite of layered double hydroxide/geopolymer for co-immobilization of  $\text{Cs}^+$  and  $\text{SeO}_4^{2-}$  from aqueous solution. *Sci. Total Environ.* **2019**, *695*, 133799. [[CrossRef](#)]
111. Skorina, T. Ion exchange in amorphous alkali-activated aluminosilicates: Potassium based geopolymers. *Appl. Clay Sci.* **2014**, *87*, 205–211. [[CrossRef](#)]
112. Abdel Rahman, R.O.; Ojovan, M.I. (Eds.) Techniques to test cementitious systems through their life cycles. In *Sustainability of Life Cycle Management for Nuclear Cementation-Based Technologies*; Woodhead Publishing: Chichester, UK, 2021; pp. 407–430. [[CrossRef](#)]
113. Varlakov, A.; Zhrebtsov, A.; Ojovan, M.I.; Petrov, V. Long-term irradiation effects in cementitious systems. In *Sustainability of Life Cycle Management for Nuclear Cementation-Based Technologies*; Woodhead Publishing: Chichester, UK, 2021; pp. 161–180.
114. Mast, B.; Gerardy, I.; Pontikes, Y.; Schroeyers, W.; Reniers, B.; Samyn, P.; Gryglewicz, G.; Vandoren, B.; Schreurs, S. The effect of gamma radiation on the mechanical and microstructural properties of Fe-rich inorganic polymers. *J. Nucl. Mater.* **2019**, *521*, 126–136. [[CrossRef](#)]
115. Yeoh, M.L.; Ukritnukun, S.; Rawal, A.; Davies, J.; Kang, B.J.; Burrough, K.; Aly, Z.; Dayal, P.; Vance, E.R.; Gregg, D.J. Mechanistic impacts of long-term gamma irradiation on physicochemical, structural, and mechanical stabilities of radiation-responsive geopolymer pastes. *J. Hazard. Mater.* **2021**, *407*, 124805. [[CrossRef](#)] [[PubMed](#)]
116. ANSI-ANS-16.1; Measurement of the Leachability of Solidified Low-Level Radioactive Waste by a Short-Term Test Procedure. American Nuclear Society: La Grange Park, IL, USA, 2003.
117. Ji, Z.; Pei, Y. Immobilization efficiency and mechanism of metal cations ( $\text{Cd}^{2+}$ ,  $\text{Pb}^{2+}$  and  $\text{Zn}^{2+}$ ) and anions ( $\text{AsO}_4^{3-}$  and  $\text{Cr}_2\text{O}_7^{2-}$ ) in waste-based geopolymer. *J. Hazard. Mater.* **2020**, *384*, 121290. [[CrossRef](#)] [[PubMed](#)]
118. Melo, L.G.A.; Periera, R.A.; Pires, E.F.C.; Darwish, F.A.I.; Silva, F.J. Physicochemical characterization of pulverized phyllite rock for geopolymer resin synthesis. *Mater. Res.* **2017**, *20*, 236–243. [[CrossRef](#)]
119. Farid, O.M.; Abdel Rahman, R.O. Preliminary assessment of modified borosilicate glasses for chromium and ruthenium immobilization. *Mater. Chem. Phys.* **2017**, *186*, 462–469. [[CrossRef](#)]
120. Kozai, N.; Sato, J.; Osugi, T.; Shimoyama, I.; Sekine, Y.; Sakamoto, F.; Ohnuki, T. Sewage sludge ash contaminated with radiocesium: Solidification with alkaline-reacted metakaolinite (geopolymer) and Portland cement. *J. Hazard. Mater.* **2021**, *416*, 125965. [[CrossRef](#)] [[PubMed](#)]
121. Abdel Rahman, R.O.; Metwally, S.S.; El-Kamash, A.M. Life Cycle of Ion Exchangers in Nuclear Industry: Application and Management of Spent Exchangers. In *Handbook of Ecomaterials*; Martínez, L., Kharissova, O., Kharisov, B., Eds.; Springer: Cham, Switzerland, 2019; Volume 5, pp. 3709–3732. [[CrossRef](#)]
122. Jang, J.G.; Lee, N.K.; Lee, H.K. Fresh and hardened properties of alkali-activated fly ash/slag pastes with superplasticizers. *Constr. Build. Mater.* **2014**, *50*, 169–176. [[CrossRef](#)]
123. Lee, N.K.; Lee, H.K. Reactivity and reaction products of alkali-activated, fly ash/slag paste. *Constr. Build. Mater.* **2015**, *81*, 303–312. [[CrossRef](#)]
124. Phillip, E.; Khoo, K.S.; Yusof, M.A.W.; Rahman, R.A. Mechanistic insights into the dynamics of radionuclides retention in evolved POFA-OPC and OPC barriers in radioactive waste disposal. *Chem. Eng. J.* **2022**, *437*, 135423. [[CrossRef](#)]
125. Pan, Y.; Bai, Y.; Chen, C.; Yao, S.; Tian, Q.; Zhang, H. Effect of calcination temperature on geopolymer for the adsorption of cesium. *Mater. Lett.* **2023**, *330*, 133355. [[CrossRef](#)]
126. Ma, S.; Yang, H.; Fu, S.; He, P.; Duan, X.; Yang, Z.; Jia, D.; Colombo, P.; Zhou, Y. Additive manufacturing of geopolymers with hierarchical porosity for highly efficient removal of  $\text{Cs}^+$ . *J. Hazard. Mater.* **2023**, *443*, 130161. [[CrossRef](#)] [[PubMed](#)]
127. El-Eswed, B.I. *Solidification Versus Adsorption for Immobilization of Pollutants in Geopolymeric Materials: A Review*; Intechopen: London, UK, 2018.
128. Abdel Rahman, R.O.; Zaki, A.A. Comparative analysis of nuclear waste solidification performance models: Spent ion exchanger-cement based wasteforms. *Process Saf. Environ. Prot.* **2020**, *136*, 115–125. [[CrossRef](#)]
129. Shi, C.; Fernández-Jiménez, A. Stabilization/solidification of hazardous and radioactive waste with alkali-activated cements. *J. Hazard. Mater.* **2006**, *137*, 1656–1663. [[CrossRef](#)] [[PubMed](#)]
130. Khalil, M.Y.; Merz, E. Immobilization of intermediate-level wastes in geopolymers. *J. Nucl. Mater.* **1994**, *211*, 141–148. [[CrossRef](#)]
131. El-Eswed, B.I.; Aldagag, O.M.; Khalili, F.I. Efficiency and mechanism of stabilization/solidification of  $\text{Pb(II)}$ ,  $\text{Cd(II)}$ ,  $\text{Cu(II)}$ ,  $\text{Th(IV)}$  and  $\text{U(VI)}$  in metakaolin based geopolymers. *Appl. Clay Sci.* **2017**, *140*, 148–156. [[CrossRef](#)]

132. Perera, D.S.; Blackford, M.G.; Vance, E.R.; Hanna, J.V.; Finnie, K.S.; Nicholson, C.L. Geopolymers for the immobilization of radioactive waste. *Mat. Res. Soc. Symp. Proc.* **2004**, *824*, 432–437. [CrossRef]
133. Jia, L.; He, P.; Jia, D.; Fu, S.; Wang, M.; Wang, M.; Duan, X.; Yang, Z.; Zhou, Y. Immobilization behavior of Sr in geopolymer and its ceramic product. *J. Am. Ceram. Soc.* **2019**, *103*, 1372–1384. [CrossRef]
134. Ke, X.; Bernal, S.A.; Sato, T.; Provis, J.L. Alkali aluminosilicate geopolymers as binders to encapsulate strontium-selective titanate ion-exchangers. *Dalton Trans.* **2019**, *48*, 12116–12126. [CrossRef]
135. Kuenzel, C.; Cisneros, J.F.; Neville, T.P.; Vandeperre, L.J.; Simons, S.J.R.; Bensted, J.; Cheeseman, C.R. Encapsulation of Cs/Sr contaminated clinoptilolite in geopolymers produced from metakaolin. *J. Nucl. Mater.* **2015**, *466*, 94–99. [CrossRef]
136. Peng, X.; Xu, Y.; Xu, Z.; Wu, D.; Li, D. Effect of simulated radionuclide strontium on geopolymerization process. *Procedia Environ. Sci.* **2016**, *31*, 325–329. [CrossRef]
137. Ofer-Rozovsky, E.; Arbel Haddad, M.; Bar-Nes, G.; Borjovitz, E.J.C.; Binyamini, A.; Nikolski, A.; Katz, A. Cesium immobilization in nitrate-bearing metakaolin-based geopolymers. *J. Nucl. Mater.* **2019**, *514*, 247–254. [CrossRef]
138. Cantarel, V.; Motooka, T.; Yamagishi, I. Geopolymers and their potential applications in the nuclear waste management field—A bibliographical study. *JAEA Rev.* **2017**, *14*.
139. Jing, Z.; Hao, W.; He, X.; Fan, J.; Zhang, Y.; Miao, J.; Jin, F. A novel hydrothermal method to convert incineration ash into pollucite for the immobilization of asimulant radioactive cesium. *J. Hazard Mater.* **2016**, *306*, 220–229. [CrossRef]
140. Al-Mashqbeh, A.; Abuali, S.; El-Eswed, B.; Khalili, F.I. Immobilization of toxic inorganic anions ( $\text{Cr}_2\text{O}_7^{2-}$ ,  $\text{MnO}_4^-$  and  $\text{Fe}(\text{CN})_6^{3-}$ ) in metakaolin based geopolymers: A preliminary study. *Ceram. Int.* **2018**, *44*, 5613–5620. [CrossRef]
141. Lichvar, P.; Rozložnik, M.; Sekely, S. Behaviour of aluminosilicate inorganic matrix SIAL during and after solidification of radioactive sludge and radioactive spent resins and their mixtures. *Amec Nucl. Slovak.* **2010**. Available online: [https://www-pub.iaea.org/MTCD/Publications/PDF/TE-1701\\_add-CD/PDF/Slovakia.pdf](https://www-pub.iaea.org/MTCD/Publications/PDF/TE-1701_add-CD/PDF/Slovakia.pdf) (accessed on 3 January 2022).
142. Jang, J.G.; Park, S.M.; Lee, H.K. Physical barrier effect of geopolymeric waste form on diffusivity of cesium and strontium. *J. Hazard. Mater.* **2016**, *318*, 339–346. [CrossRef] [PubMed]
143. Wang, G.; Wang, X.; Chai, X.; Liu, J.; Deng, N. Adsorption of Uranium (VI) from aqueous solution on calcined and acid-activated kaolin. *J. Appl. Clay Sci.* **2010**, *47*, 448–451. [CrossRef]
144. Künzel, C. Metakaolin Based Geopolymers to Encapsulate Nuclear Waste. Ph.D. Thesis, Imperial College, London, UK, 2013.
145. Jiang, Z.; Xu, Z.H.; Shuai, Q.; Li, P.; Xu, Y.H. Thermal stability of geopolymer—Sr contaminated zeolite A blends. *Key Eng. Mater.* **2017**, *727*, 1089–1097. [CrossRef]
146. Boškovi, I.V.; Nenadovi, S.S.; Kljajevi, L.M.; Vukanac, I.S.; Stankovi, N.G.; Lukovi, J.M.; Vukčević, M. Radiological and physico-chemical properties of red mud based geopolymers. *Nucl. Technol. Rad. Prot.* **2018**, *33*, 188–194. [CrossRef]
147. Abdel Rahman, R.O.; Ojovan, M.I. (Eds.) Sustainability of cementitious structures, systems, and components (SSC's): Long-term environmental stressors. In *Sustainability of Life Cycle Management for Nuclear Cementation-Based Technologies*; Elsevier-Woodhead Publishing: Chichester, UK, 2021; pp. 181–232.
148. De Oliveira, L.B.; de Azevedo, A.R.; Marvila, M.T.; Pereira, E.C.; Fediuk, R.; Vieira, C.M.F. Durability of geopolymers with industrial waste. *Case Stud. Constr. Mater.* **2022**, *16*, e00839. [CrossRef]
149. Kishore, Y.S.N.; Nadimpalli, S.G.D.; Potnuru, A.K.; Vemuri, J.; Khan, M.A. Statistical analysis of sustainable geopolymer concrete. *Mater. Today Proc.* **2022**, *61*, 212–223. [CrossRef]
150. Oyebisi, S.; Olutoge, F.; Kathirvel, P.; Oyaotuderekumor, I.; Lawanson, D.; Nwani, J.; Ede, A.; Kaze, R. Sustainability assessment of geopolymer concrete synthesized by slag and corncob ash. *Case Stud. Constr. Mater.* **2022**, *17*, e01665. [CrossRef]
151. Mishra, J.; Nanda, B.; Patro, S.K.; Krishna, R.S. Sustainable Fly Ash Based Geopolymer Binders: A Review on Compressive Strength and Microstructure Properties. *Sustainability* **2022**, *14*, 15062. [CrossRef]

**Disclaimer/Publisher's Note:** The statements, opinions and data contained in all publications are solely those of the individual author(s) and contributor(s) and not of MDPI and/or the editor(s). MDPI and/or the editor(s) disclaim responsibility for any injury to people or property resulting from any ideas, methods, instructions or products referred to in the content.